



## MATERIALS SCIENCE

# Surface engineering toward stable lithium metal anodes

Gongxun Lu<sup>1†</sup>, Jianwei Nai<sup>1\*</sup>, Deyan Luan<sup>2</sup>, Xinyong Tao<sup>1\*</sup>, Xiong Wen (David) Lou<sup>3\*</sup>

The lithium (Li) metal anode (LMA) is susceptible to failure due to the growth of Li dendrites caused by an unsatisfied solid electrolyte interface (SEI). With this regard, the design of artificial SEIs with improved physicochemical and mechanical properties has been demonstrated to be important to stabilize the LMAs. This review comprehensively summarizes current efficient strategies and key progresses in surface engineering for constructing protective layers to serve as the artificial SEIs, including pretreating the LMAs with the reagents situated in different primary states of matter (solid, liquid, and gas) or using some peculiar pathways (plasma, for example). The fundamental characterization tools for studying the protective layers on the LMAs are also briefly introduced. Last, strategic guidance for the deliberate design of surface engineering is provided, and the current challenges, opportunities, and possible future directions of these strategies for the development of LMAs in practical applications are discussed.

## INTRODUCTION

Modern society depends highly on high-performance electrochemical energy storage systems, battery for example, for portable electronic devices and the successful transition to renewable energy sources and electrified transportation (1, 2). Li metal has been regarded as the most promising battery anode material owing to its ultrahigh theoretical specific capacity (3860 mAh g<sup>-1</sup>), light weight (6.94 g mol<sup>-1</sup>), and the lowest redox potential (−3.04 V versus standard hydrogen electrode) (3). Despite these unique advantages, the practical application of lithium metal batteries (LMBs) is still severely hindered by Li dendrite growth, resulting in poor cycling performance and safety concerns (4).

Although various theories have been developed to unravel the mechanism of Li dendrite growth, including the nucleation and diffusion model, space-charge model, and stress-driven model (1, 5), it is recognized that Li dendrites are generally induced by an unsatisfied solid electrolyte interface (SEI) (6, 7). Because of the intrinsic ultrahigh chemical reactivity and thermodynamic instability of metallic Li, a passivation SEI layer is produced between Li metal and the electrolyte via spontaneous irreversible reactions (8). Nevertheless, the electrolyte-derived SEI is nonuniform and fragile, which induces inhomogeneous ion diffusion and the Li dendrite growth. The proliferating dendrite growth would result in continuous SEI breakage/reformation under the tremendous volume change of the Li metal anodes (LMAs) during the cycling, leading to the increase of interfacial Li<sup>+</sup> ion diffusion resistance and higher voltage polarization (9, 10). In addition, because of the preferential dissolution at the dendrite base and the potential separation of Li dendrites from the current collector, the generation of residual inactive Li ("dead Li") markedly decreases the coulombic efficiency (CE), resulting in unsatisfactory cycling performance and eventual cell

failure (11, 12). Therefore, a stable interface between the Li metal and the electrolyte is perceived as the primary premise for a working LMB.

Precise control over the composition and properties of the SEI is desired to overcome the chemical and mechanical instabilities at the electrode/electrolyte interface, thereby achieving stable and high-performance LMAs (13, 14). A rationally designed artificial SEI positioned at the Li-electrolyte interface is thought to be a promising and efficient approach due to its high feasibility and simplicity in processing. Ideally, artificial SEIs should have the following desirable characteristics (15, 16): (i) superior chemical and electrochemical stability with electronic insulation to impede continuous electrolyte decomposition and Li consumption; (ii) high mechanical modulus and flexibility to suppress the dendrite growth and restrain the volume change during the repeated cycles; and (iii) high ionic conductivity and ability to allow homogeneous Li<sup>+</sup> ion transport across the layer. In regard to the application of solid-state electrolyte (SSE) for LMAs, the design of an artificial SEI with more softness and stickiness to achieve intimate contact between the electrode and the SSE is an imperative criterion. Therefore, actively influencing and managing these features are critical for the development of advanced LMAs (17). Investigating the formation and manipulation of so-called artificial SEIs has been recognized as a rising research trend (18, 19). The development of such a functional layer requires an in-depth understanding of the relationship between its structure (morphology and composition) and its basic function in a battery cell (20). Rationally building an artificial SEI, including organic, inorganic, or hybrid one, is attracting more attention, giving rise to an opportunity to avoid continuous electrolyte decomposition and Li consumption to obtain a safe and highly stable LMA.

Surface and interface engineering has been found to play a key role in improving the electrochemical performance of LMAs by its strong capability of constructing various functional artificial SEIs (16, 21–26). As the physical/chemical properties of these artificial SEIs are essentially determined by the process of surface engineering, the states of matter (solid, liquid, and gas) of the reagents used for surface engineering deserve to be carefully considered. This is

<sup>1</sup>College of Materials Science and Engineering, Zhejiang University of Technology, Hangzhou 310014, China. <sup>2</sup>School of Chemical and Biomedical Engineering, Nanyang Technological University, 62 Nanyang Drive, Singapore 637459, Singapore. <sup>3</sup>Department of Chemistry, City University of Hong Kong, 83 Tat Chee Avenue, Kowloon, 999077, Hong Kong, China.

<sup>†</sup>These authors contributed equally to this work.

\*Corresponding author. Email: jwnai@zjut.edu.cn (J.N.); tao@zjut.edu.cn (X.T.); david.lou@cityu.edu.hk (X.W.L.)

because different reagents will inevitably lead to variations in the structure and physicochemical properties of the formed artificial SEIs. For example, a solid reagent has a rigid structure and a stable, distinct shape that can only be altered through external force. These properties lead to poor interfacial contact between the solid reagents and the Li metal unless a spontaneous chemical reaction could occur on their interface. As compared to the solid, the molecules in the liquid reagents have a certain capacity to move around, which allows them a more intimate contact with the Li metal and diverse options for the SEI's structures. As opposed to the solids and liquids, the atoms/molecules in the gas reagents have much higher kinetic energy due to their higher dispersity and smaller intermolecular force, endowing them with an improved chemical reaction kinetic with the Li metal.

This review summarizes recent efforts aimed at implementing surface engineering that involves pretreatment protocols before the stage of battery assembly on the LMAs to address the structural and electrochemical requirements for high-performance artificial SEIs. The surface engineering techniques are mainly categorized by the states of matter (solid, liquid, and gas) of the reagents used to pretreat the LMAs (Fig. 1). The category of using some peculiar pathways (plasma for example) is also included. Moreover, we will discuss the fundamental characterization techniques for elucidating

the formation mechanism and physicochemical properties of these as-formed artificial SEIs. Last, potential future research directions regarding the rational design of surface engineering and advanced characterization tools for LMAs will be outlooked.

## SURFACE PRETREATMENT STRATEGIES

### Solid-phase pathways

Since the SEI is made up of solids, the solid-phase approach is the simplest and most direct strategy to pretreat the surface of the LMAs, where researchers commonly just replace or enhance the naturally formed SEI by another predesigned solid. In this regard, three representative surface pretreatment processes are introduced as follows.

### Mechanical processing

Mechanical processing is a simple, processable, and cost-effective process to realize dendrite-free LMAs (27, 28). The highly ductile Li metal can be easily molded or deformed to form surface patterns by large mechanical strains. The patterned surface could decrease the current density over the Li metal surface and diminish Li dendrite formation during cell operation by expanding the surface area of Li metal.

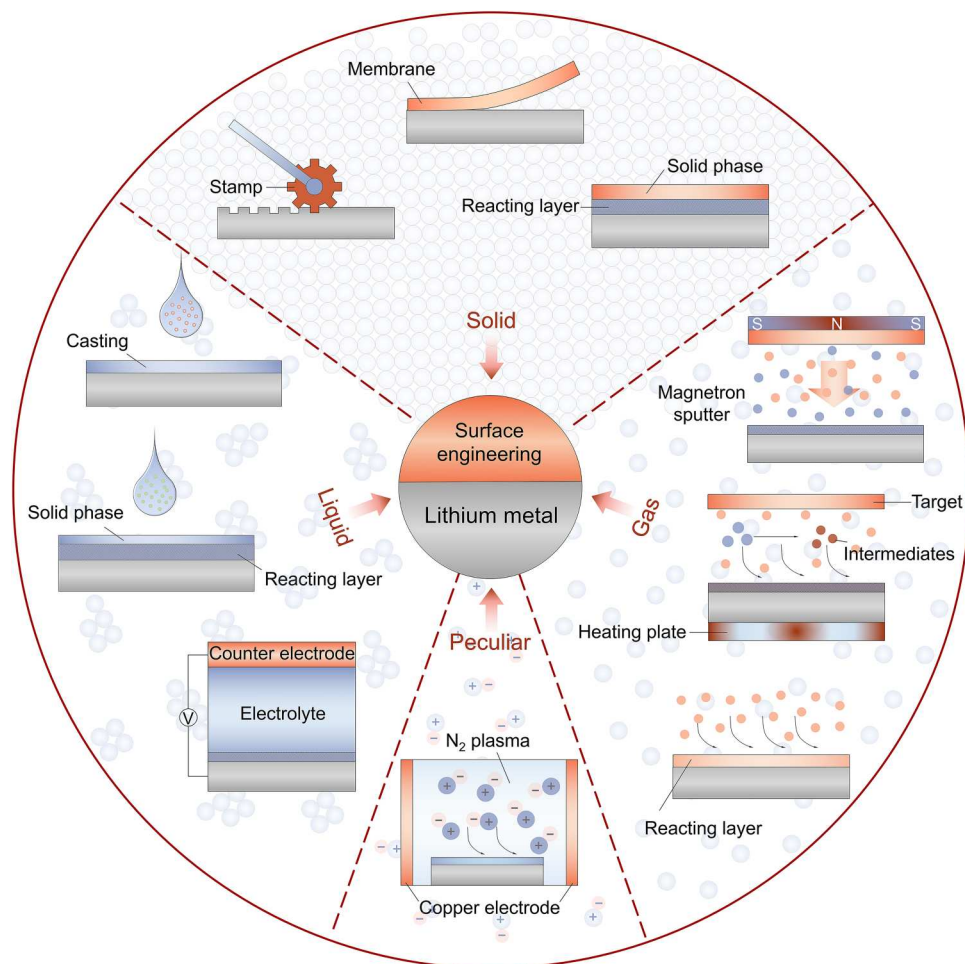


**Fig. 1. Schematic illustration of the current surface engineering strategies for stabilizing LMAs.**

Stamp is an effective mechanical processing technique to construct surface patterns. In 2014, Ryou *et al.* (29) pioneered the use of skin needling for surface roughening to construct a large-surface area LMA with an abundance of Li plating sites. The microneedled Li metal with lower charge transfer resistance provided better electrochemical performance than bare Li. Motivated by the simplicity and effectiveness of this technique, Park *et al.* (30) demonstrated the possibility of employing a surface-patterned Li metal (spLi) pretreated with a commercially available microneedle roller in secondary batteries (Fig. 2A). They systematically verified the relationship between the pattern dimension and Li deposition behavior with the help of finite element analysis and postmortem analysis. After the stamping process, the spLi could be reversibly plated and stripped without Li dendrite growth in the surface-patterned holes. Creating a micro-sized array for guiding the Li plating/stripping behavior by micropattern stamping technique is another approach for stabilizing LMAs (31). In addition, a three-dimensional (3D) stainless-steel

mesh and copper net-modified Li metal interlayer was used to stabilize LMAs (32–34).

The mechanical processing approach is viable because it is economical, reproducible, and applicable to mass production lines. Nonetheless, there are two limitations: (i) The capacity for Li plating without the formation of Li dendrites is highly dependent on the size of the holes. When the deposited Li exceeds the amount that can be accommodated in the holes, Li metal will grow out of the holes and become dendrites. (ii) Without a preset protecting layer on Li metal, the microneedled Li will convert into 2D Li foil and fail to suppress dendritic Li growth during a long cycling test.

### Membrane modification

Apart from the direct physical treatment of the Li metal, applying as-prepared free-standing films as the artificial SEIs would be an interesting approach to enhance the electrochemical performance of LMAs. The as-prepared film composed of inorganic components exhibits excellent chemical stability against Li metal and physically suppresses dendrite formation. Carbon-based materials are frequently adopted as such inorganic materials. For example, Zheng *et al.* (18) first reported a monolayer of interconnected amorphous hollow carbon nanospheres as an artificial SEI to isolate Li metal from the electrolyte. In addition, Kim *et al.* (35) used phosphate-functionalized reduced graphene oxides (rGO) to create Langmuir-Blodgett artificial SEIs (LBASEIs) on the surface of LMAs (Fig. 2B). The effectiveness of the LBASEI is primarily from its ability to regulate the electromigration. As a result, a LBASEI-modified 20- $\mu\text{m}$  LMA paired with the  $\text{Li}[\text{Ni}_{0.8}\text{Co}_{0.1}\text{Mn}_{0.1}]\text{O}_2$  (NCM811) cathode (negative/positive capacity ratio of around 1) was used to construct a full cell with superior cycling performance of over 200 cycles. Moreover, Li *et al.* (36) proposed a self-assembled rGO layer on LMA to achieve planar Li via in-plane lattice matching between the Li metal and the rGO.

3D structured SEIs have been used to alleviate the volume change and minimize the damage to the SEI during cycling. For instance, Cheng *et al.* (37) demonstrated an effective strategy to realize a dendrite-free LMA by using 3D glass fibers with large quantities of polar functional groups as the artificial SEIs (Fig. 2C). The polar functional groups of the glass fibers can offer strong interaction with  $\text{Li}^+$  ions, which induced a homogeneous  $\text{Li}^+$  ion flux and prevent the accumulation of  $\text{Li}^+$  ions around protuberances of Cu foil. Moreover, Zhai *et al.* (38) presented the design of a 3D architecture constructed by g- $\text{C}_3\text{N}_4$ /graphene/g- $\text{C}_3\text{N}_4$  sandwiched nanosheets to guide homogeneous Li deposition. Its uniform lithiophilic sites and nanopore channels enable uniform Li plating between the graphene and g- $\text{C}_3\text{N}_4$ , prohibiting direct contact of the electrolyte with the Li metal. In addition, diverse inorganic protective layers, such as  $\text{Cu}_3\text{P}$  (39), carbon nanotube (CNT) film (40), graphene (41),  $\text{Li}_3\text{OCl}$  (42), aluminum silicate (43),  $\text{Mo}_6\text{S}_8/\text{C@Li}$  (44), and  $\alpha\text{-Si}_3\text{N}_4$  (45), have been proposed to directly coated on the LMAs to solve the notorious surface problem.

Organic coating layers with superior mechanical deformability and low density are promising candidates to stabilize LMAs. For example, a modified polydimethylsiloxane (PDMS) film with nanopores has been used to improve the cycling stability of LMAs (46). The nanopores of the PDMS film show efficient  $\text{Li}^+$  ion transport, mechanical and chemical stability, and compatibility with different electrolytes. Moreover, a functional soft polymer with highly viscoelastic properties in the coating layer imparts a homogenizing effect

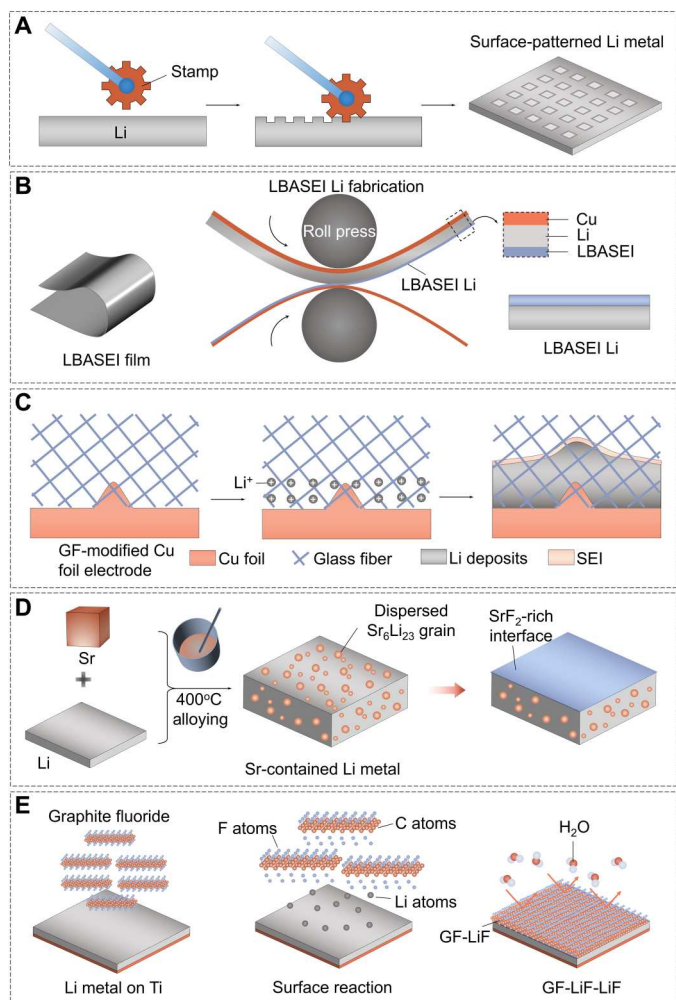


**Fig. 2. Schematic illustration of surface pretreatment using solid-phase pathways.** (A) The stamp modified process on Li metal. (B) Fabrication of the LBASEI Li via a roll-press process. (C) The glass fiber cloth is directly coated on copper foil to render the dendrite-free Li deposits. (D) The schematic diagram for the fabrication of the Li-Sr anode via a high-temperature alloying process. (E) Schematic illustration of GF-LiF-Li preparation and its protective effect for LMAs.



on the  $\text{Li}^+$  ion flux to prevent rapid dendrite formation at hotspots in the SEI during cycling (47). Because of the trade-off between the Young's modulus and toughness of a traditional polymer, the fixed cross-linking networks may break during stretching. To solve this problem, a tough polymer with a slide-ring structure as a self-adaptive layer was introduced on the LMAs (48). The slide-ring polymer with a dynamically cross-linked network moves freely while maintaining its toughness and fracture resistance, which allows it to dissipate the tension induced by the growth of the Li dendrites. Other reported organic protective layers, such as N-doped polyacrylonitrile fiber (49), nanoporous polyether sulfone (50), and clay/cross-linked network polymer (51), all have high ionic conductivity, resulting in a dendrite-free and stable LMA.

Mimicking the "early warning" defense responses in biological immunization mechanisms, Wang *et al.* (52) proposed that the fibroin molecules can work as an artificial SEI to prevent Li dendrite growth. The protein molecules are preferably adsorbed on the tips of Li buds through spatial conformation and secondary structure transformation from  $\alpha$ -helix to  $\beta$ -sheets. This affects the local electric field intensity around the tips of Li buds and results in uniform Li plating and stripping during cycling. Moreover, biomineralization is a widespread phenomenon in nature leading to the formation of hierarchically structured minerals by living organisms (53). Inspired by the calcified crystallization on the eggshell membrane, Ju *et al.* (54) introduced a biomacromolecule matrix obtained from the natural membrane of eggshell to realize a dendrite-free LMA, and the regulatory mechanism was revealed by atomic-resolution cryo-transmission electron microscopy (cryo-TEM). The naturally soluble chemical species in the biomacromolecules was found to be able to participate in the formation of the SEI upon cycling, thus effectively enhancing the electrochemical performance.

Organic-inorganic composite layers with associated strengths from the organic and inorganic components have been presented to simultaneously provide fast  $\text{Li}^+$  ion diffusion, high modulus, and good shape conformability (55). For example, a poly(vinylidene-co-hexafluoropropylene) (PVDF-HFP) organic matrix with rigid LiF particles has been hybridized into a film, which serves as an artificial SEI on LMAs (56). To construct a protective layer with an ionic shielding property, Kim *et al.* (57) fabricated Li-terminated sulfonated titania-coated Li (LTST-Li) via direct transfer to Li using a roll-press machine. As a result, the LTST-Li anodes have high conductivity at the interface and high physical and chemical stability to shield the Li metal, which can stabilize electrochemical processes at both the anode and cathode of Li-S cells.

Note that the thickness of the as-prepared membrane is normally greater than a few micrometers, implying that the total volume energy density of the LMA would be sacrificed. In addition, the as-prepared membrane added onto the surface of Li metal can hardly manage the homogeneity of the SEI during the cycling, which may result in high electrochemical polarization.

### Chemical reaction with solids

Designing a chemical reaction between metallic Li and solids has been reported to be an effective method to build an artificial SEI with high ionic conductivity and high mechanical property. Li-rich alloys have high  $\text{Li}^+$  ion diffusion coefficients and have proven to be beneficial in improving  $\text{Li}^+$  ion diffusion at the electrode/electrolyte interface (58, 59). For instance, a Li and Li-Sn alloy ( $\text{Li}_{22}\text{Sn}_5$ ) integrated 3D networks have been in situ formed through

the spontaneous reaction between periodically stacked nanolayers of Li and Sn (60). Such a 3D nanostructured  $\text{Li}_{22}\text{Sn}_5$  network enables ultrafast charger diffusion across the entire electrode and inhibits the volume expansion during Li stripping/plating processes. A Li-Sr alloy electrode with a designed composition of 11 weight % (wt %) Sr was synthesized by heating and stirring Li and Sr metals at 400°C in a glovebox (Fig. 2D) (61). When the battery is cycling, a  $\text{SrF}_2$ -rich SEI can be generated in fluoride-rich electrolytes. The  $\text{SrF}_2$ -rich SEI enables outstanding cycling performance and improved CE of the Li-Sr anode in the half cell at an ultrahigh current density of 30  $\text{mA cm}^{-2}$ .

In addition to this alloy-derived SEI, some researchers have focused on constructing LiF-based protective layers on LMAs via a direct reaction between inorganic nonmetallic materials and Li metal, which enables a high mechanical modulus and high ionic conductivity (62). For example, a modified Li metal is fabricated by incorporating graphite fluoride (GF) in molten Li at 250°C (Fig. 2E) (63). The Li bonds strongly with the GF to form a LiF layer. The obtained GF-LiF-Li composite can sustain its initial structure in a humid air. In addition, this composite can prevent the parasitic reaction between Li metal and organic solvents owing to its hydrophobicity. As a result, the GF-LiF-Li can exhibit comparable electrochemical performance to bare LMA even after exposure to a moist atmosphere with a relative humidity of 20 to 35% for over 24 hours. In addition, a multifunctional complementary LiF-rich protective layer was formed on an LMA through in situ reaction of metallic Li with poly(tetrafluoroethylene) (64, 65). This gradient protective layer integrates the homogenizing function of the F-doped carbon for  $\text{Li}^+$  ion flux and the fast  $\text{Li}^+$  ion diffusion ability of LiF. Furthermore, a fluorinated protective layer with high ionic conductivity has been constructed in situ through a solid-state anodic oxidation method. The as-prepared F-rich protective film efficiently suppresses dendrite growth and promotes the electrochemical performance of the LMB in a commercial ester electrolyte (66).

In addition to LiF,  $\text{Li}_3\text{N}$  and  $\text{Li}_3\text{P}$  components have been demonstrated to suppress the formation of Li dendrites due to their high ionic conductivity and high mechanical modulus. For example, Ye *et al.* (67) reported that in a simple hyperthermal reduction process,  $\text{g-C}_3\text{N}_4$  powder can react with molten Li to form a composite N-organic/ $\text{Li}_3\text{N}$  artificial SEI on the surface of Li metal. Lee *et al.* (68) reported that  $\text{Cu}_3\text{N}$  nanowires (NWs) was conformally printed onto the surface of Li metal through a one-step roll pressing to form a  $\text{Li}_3\text{N}@Cu$  NW layer. The  $\text{Li}_3\text{N}@Cu$  NW layer can assist homogeneous  $\text{Li}^+$  ion flux with the 3D channel structure and a high  $\text{Li}^+$  ion conductivity from the  $\text{Li}_3\text{N}$ , which enhances the reversible Li plating/stripping behavior. In addition, an interconnected  $\text{Li}_3\text{P}@Cu$  layer activated by the interfacial reaction between  $\text{Cu}_3\text{P}$  arrays and Li metal has been efficiently constructed on the surface of Li foil through a room-temperature mechanical rolling process (69). It is demonstrated that  $\text{Li}_3\text{P}$  could reduce the diffusion barrier of  $\text{Li}^+$  ions to ensure a well-dispersed current density.

### Liquid-phase pathways

Taking advantage of the fluidity of liquids and its ability to dissolve chemicals or disperse the colloid materials, a uniform and component-tunable artificial SEI could be constructed on the surface of the LMAs via the liquid-phase strategy (22, 70). Therefore, direct contact between the LMA and electrolyte after the battery assembly

could be restricted by this preformed artificial SEI, leading to a decreased consumption of the electrolyte and Li metal, preventing heterogeneous Li deposition, and suppressing the dendrite formation (24).

### Solution casting

The solution-casting method, including immersion, drop coating, doctor blading, and spin coating, has been developed as a facile and reproducible way to create functional barrier layers to avoid the drawbacks of electrolyte-derived SEIs (Fig. 3A). Many of the presynthesized materials, including organic, inorganic, and the organic-inorganic composite, could be easily coated on the LMAs without any chemical reaction, efficiently enhancing the mechanical strength of the SEI to block Li dendrites and enabling homogeneous  $\text{Li}^+$  ion flux across the coating layer with the controllable interfacial resistance.

Organic coating layers with superior mechanical deformability and low density are promising candidates to stabilize LMAs (71). In 1993, Takehara (72) pioneered the construction of a stable thin polymer film on the surface of Li metal by plasma-triggered polymerization of a liquid mixture. Thereafter, many researchers developed the polymer protective film on the Li surface via in situ polymerization, triggered polymerization, or direct coating. Recently, Zhao *et al.* (73) have spin-coated a mechanically interlocked network (MIN) on the surface of LMA under the argon atmosphere, followed by an ultraviolet-assisted polymerization to fabricate a MIN interfacial layer. The unique energy dissipation capability of the MIN layer could help the LMA survive from repeated volume variation during long-term cycling. In addition, Gao *et al.* (74) proposed a skin-grafting strategy that stabilizes the SEI and regulates

the Li deposition/dissolution behavior by direct coating a chemical-ly and electrochemically active polymer layer on the surface of Li metal. This layer contains cyclic ether groups with a stiff polycyclic main chain, incorporating ether-based polymeric components into the durable SEI. Furthermore, a polycationic and hydrophobic polymer protective layer built by a scalable tape-casting method has been developed to enable dendrite-free LMAs (75). The polymeric cations of poly(diallyl dimethyl ammonium) and bis(trifluoromethanesulfonyl)imide (TFSI) anions could provide a uniform  $\text{Li}^+$  ion flux at the coated LMA and a hydrophobic property, which improves homogeneous Li plating/stripping and moisture stability under air condition. In addition, Yang *et al.* (76) proposed a fluid fluorinated coating layer to stabilize LMAs and regulate Li plating by dripping a perfluoropolyether oil drop onto the surface of Li metal. The obtained SEI is reinforced with rich C-F and Li-F components, leading to homogeneous Li deposition and compact interconnected network morphology. Moreover, several stable PVDF and cross-linked PVDF-HFP films have also been formed on the Li metal surface via a simple casting method for prominent cycling performance (77, 78).

Carbonaceous materials including CNTs, graphene, and its derivatives are promising inorganic materials that can meet the requirements for artificial SEI due to their superior mechanical properties (79, 80). In addition, the mechanical and electronic properties of graphene can be selectively tuned or modified via proper functionalization and introduction of structural defects. For instance, GO layers have been coated onto LMAs to suppress dendrite formation and enhance cycling stability through a drop-casting process (81). Furthermore, 2D rGO layers have been coated on Li metal by a solvent evaporation-assisted self-assembly method

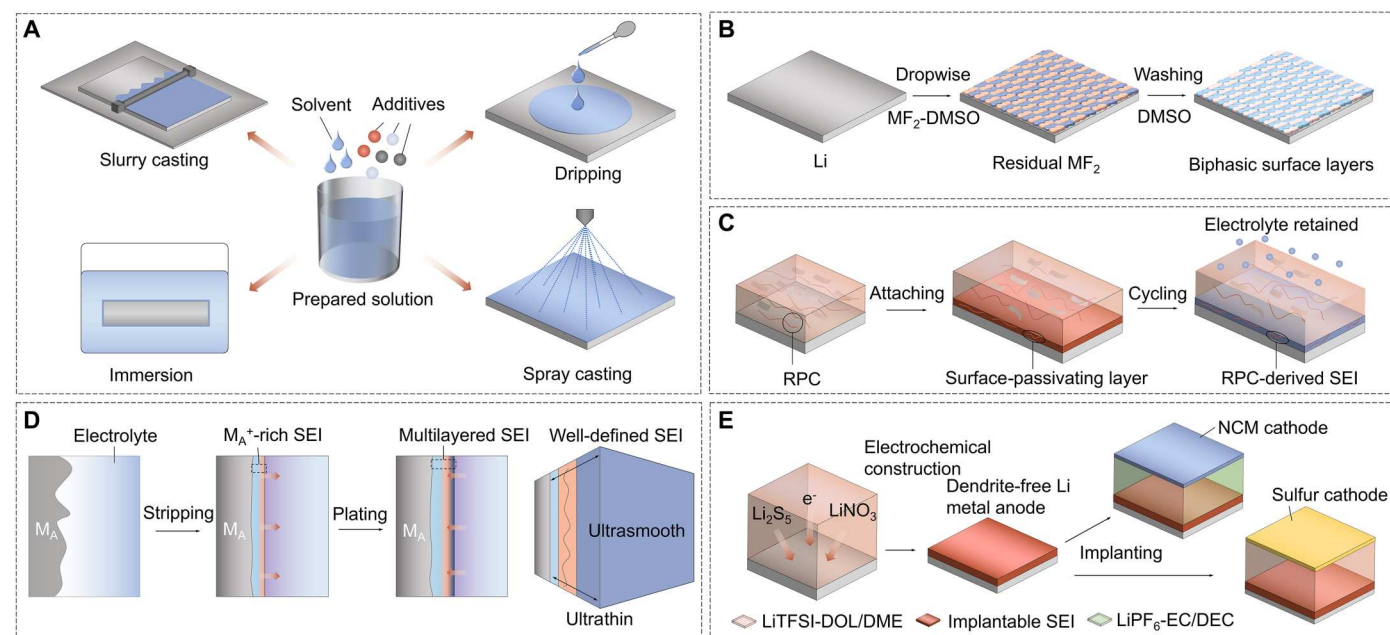


**Fig. 3. Schematic illustration of surface pretreatment using liquid-phase pathways.** (A) Surface processing strategies via various solution casting methods, including slurry casting, immersion, dripping, and spray casting. (B) High-polarity DMSO was selected to dissolve sufficient metal fluorides (e.g.,  $\text{SnF}_2$ ,  $\text{InF}_3$ , and  $\text{ZnF}_2$ ), which is crucial to forming the uniform and robust BSLs on Li metal. (C) Design of a polymer-inorganic SEI using the RPC precursor rather than the electrolyte to trigger a chemical reaction with Li. (D) Potentiostatic stripping and galvanostatic plating for polishing of and formation of SEI on metal anode (MA) surface. (E) Ex situ SEI construction on the Li plate by electrochemical methods in 1.0 M LiTFSI-DOL/DME electrolyte with 0.02 M  $\text{Li}_2\text{S}_5$ –5.0 wt %  $\text{LiNO}_3$  hybrid additives.

(79). "Defect-free" graphene has also been synthesized via a special flow-aided sonication exfoliation method, allowing direct comparison of Li deposition behavior and electrochemical performance with those of common rGO (80). Moreover, a promising gradient layer with a lithiophobic CNT layer at the top and a lithiophilic ZnO-coated CNT layer at the bottom has been constructed on the surface of Li metal (82). The lithiophilic-lithiophobic gradient layer can stabilize the SEI and successfully suppress dendrite growth during Li plating/stripping.

Many researchers have developed special strategies to protect LMAs by a composite protective layer, which is composed of inorganic nanoparticles and a plastic polymer, effectively improving the SEI stability and inhibiting Li dendrite growth. An  $\text{Al}_2\text{O}_3$ /PVDF-HFP composite layer has been used as an artificial SEI because of its high mechanical properties and fast  $\text{Li}^+$  ion transport, resulting in a notable enhancement in the electrochemical performance of LMAs (83). A graphene-polydopamine composite has been introduced as a stable protective layer onto LMAs to inhibit Li dendrite growth and prevent parasitic reactions between Li metal and electrolyte (84). Inspired by the phenomenon that membrane proteins can selectively transport alkali ions across cell membranes, the building of biomimetic protective membranes with glutamate-like ionic channels for LMAs is expected to deliver an improved performance. A stable artificial SEI has been rationally designed and coated on the surface of Li metal by applying the  $\text{ClO}_4^-$ -decorated metal-organic framework (MOF) via drop-casting (85). The  $\text{UO}-66\text{-ClO}_4/\text{Li-Nafion}$  composite layer exhibits excellent mechanical strength, high  $\text{Li}^+$  ion mobility, and uniform  $\text{Li}^+$  ion flux, which can successfully restrain unnecessary reactions of the Li metal with the electrolyte and formation of fragile SEIs. Fan *et al.* (86) reported a similar work on polyvinyl alcohol cementing a Zn-MOF as a stable protective layer for homogeneous  $\text{Li}^+$  ion transport, suppressing Li dendrite growth, and reducing the volume change. Furthermore, a robust SEI with high  $\text{Li}^+$  ion transport efficiency and high stability has been rationally constructed by drop casting of 2D anionic covalent organic frameworks (ACOFs) (87). The ACOF layer served as an SEI offers strong affinity and fast translocation pathways for  $\text{Li}^+$  ions, thereby supporting ionically selective penetration into the liquid electrolyte and giving high conductivity of at least  $3.7 \text{ mS cm}^{-1}$ .

### Chemical reaction with liquids

Owing to the high reactivity of metallic Li, redox reactions can occur between Li and the liquid reagents, in situ generating an artificial SEI with much more intimate contact to the LMAs. Therefore, the method of chemical reaction with liquids offers the possibility of fine control of the composition and realization of gradient structure of the artificial SEIs according to the requirements.

The organic layers have a flexible nature, so they can mechanically accommodate the volume changes of LMA to a large extent (88). Some researchers reported an extremely simple method of constructing a protective layer on a Li metal surface via chemical reactions between Li metal and 1,4-dioxacyclohexane or 1,3-dioxolane (DOL) (89, 90). Moreover, to build a stable protective layer, researchers have immersed Li metal in fluoroethylene carbonate solvent to generate a passivation layer via spontaneous decomposition of the solvent (91, 92). The obtained artificial SEIs can protect the LMA from the corrosion of electrolytes and regulate the homogeneous plating of Li to achieve a dendrite-free LMA. Many other

polymer layers can be formed on LMAs via in situ chemical reactions with metallic Li using polymers such as polyphosphoric ester, polyacrylic acid, polylactic acid and poly(ethylene oxide) (PEO) (93–95). To achieve long-term Li plating/stripping cycling at high current densities and high areal capacity, Wang *et al.* (95) designed a self-healable supramolecular copolymer (termed PEO-UPy) coating layer for providing diffusion pathways for  $\text{Li}^+$  ion transport, enabling uniform Li deposition during cycling. As a result, the LiPEO-UPy-coated LMA endows dendrite-free Li deposition at an ultrahigh current density of  $20 \text{ mA cm}^{-2}$  over 4000 cycles in symmetrical cells.

Commonly, inorganic protective layers have relatively high  $\text{Li}^+$  ions conductivity and Young's modulus, which could physically suppress dendrite growth (96). For instance, Bai *et al.* (97) reported a simple and universal process to develop spontaneously reduced graphene (SR-G) directly coated on alkali metals (e.g., Li, Na, and K) under moderate conditions. The symmetric cell of SR-G-coated Li displays an ultralong life span of over 1000 cycles at a high current density of  $5 \text{ mA cm}^{-2}$  in carbonate electrolyte. Apart from the carbonaceous materials, lithium-based inorganic compounds with high ionic conductivity have been proven to be promising protective layers to suppress the growth of dendritic Li. For instance,  $\text{Li}_2\text{S}$  has outstanding chemical stability against Li and the lowest formation energy among lithium polysulfides. Therefore, a high-quality SEI layer containing inorganic  $\text{Li}_2\text{S}$  nanoparticles was constructed on LMAs via a simple reaction between Li and  $\text{CS}_2$  solution with 5 wt % S dissolved (98). Moreover, a thin  $\text{Li}_3\text{PS}_4$  layer was fabricated by an in situ reaction between  $\text{P}_4\text{S}_{16}$  and Li in "N-methyl-2-pyrrolidone solvent (99). Recently, a  $\text{Li}_3\text{PO}_4$ - $\text{Li}_3\text{N}$  hybrid layer was also constructed on LMAs via a  $\text{LiNO}_3/\text{H}_3\text{PO}_4$  pretreatment process (100).

In 2017, Liang *et al.* (101) reported that a series of Li-rich composite alloy films (such as  $\text{Li}_{13}\text{In}_3$ ,  $\text{LiZn}$ ,  $\text{Li}_3\text{Bi}$ , and  $\text{Li}_3\text{As}$ ) can be synthesized by reacting Li with lithium-based compounds. These alloys can potentially prevent the Li dendrite growth, which is attributed to the synergy of fast  $\text{Li}^+$  ion migration through Li-rich ion conductive alloys coupled with an electronically insulating surface component. Furthermore, more Li-rich alloy layers have been conducted on the surface of Li metal (102–104). For example, a polymer/alloy hybrid protective layer, consisting of polymer and LiF-rich Li-Sb alloy, was formed by an in situ chemical reaction process (103). The  $\text{Li}_3\text{Sb}$ -LiF hybrid layer displays a superionic conductivity and electron-blocking capability to reduce the electron tunneling from the LMA into the SEI. A stable biphasic surface layer (BSL) was developed by a simple pretreatment reaction between Li metal and metal fluoride dissolved in the dimethylsulfoxide (DMSO) solution (Fig. 3B) (104). The obtained BSL is composed of lithiophilic alloy and LiF phase on Li metal, which prohibits the shuttle effect and improves the cycling stability of Li-S batteries, enabling fast  $\text{Li}^+$  ion transport and suppressing dendrite growth. Recently, gallium-based liquid metal (LM) alloys (such as Ga and  $\text{GaInSn}$ ) have attracted some attention for the similar functionality as the alloys mentioned above. Moreover, these Ga-based LM alloys have unique properties beyond the solid ones, including good fluidity, low melting point, nontoxicity, high surface tension, and high electrical/thermal conductivities (105, 106).

To overcome some disadvantages arising from the single organic or inorganic layer, the strategy of building organic-inorganic



composite layers has been proposed to take advantage of the merits of both components via spontaneous chemical reactions between the LMAs and liquids (107). A composite containing multiple components of polymer-tethered organo(poly)sulfide, inorganic  $\text{Li}_3\text{PS}_x$ , Li sulfides, and Li salts was designed as a multifunctional artificial SEI on the surface of Li metal (108). A stable hybrid SEI, composed of Si-interlinked OOCOR molecules and LiCl salt, was conducted on the LMA by in situ synthesis that uses readily accessible  $\text{SiCl}_4$  cross-linking chemistry (109). In particular, Gao *et al.* (110) described a molecule-level SEI design based on a reactive polymer composite (RPC), which can effectively reduce the electrolyte decomposition during SEI creation and maintenance (Fig. 3C). Combined cryo-TEM, atomic force microscopy (AFM), and surface-sensitive spectroscopy investigations revealed that the SEI layer is composed of polymeric Li salt, LiF nanoparticles, and GO sheets. The compact RPC-derived SEI exhibits excellent passivation, uniformity, and mechanical strength. Under lean electrolyte, limited Li excess, and high-capacity conditions, the polymer-inorganic SEI permits dendrite-free Li deposition with excellent efficiency and stable cycling of 4-V Li/NCM523 cells.

### Electrochemical treatment

The electrochemical treatment process has been proposed to fabricate ideal SEIs under a dedicatedly designed electrochemical environment with specific parameters (including electrolyte formulation, voltage, operating temperature, etc.) (16, 111). As a result, these electrochemically constructed SEIs have more sophisticated components and structures as compared to single- (or dual-) component protective coatings synthesized by direct coating or regular chemical pretreatment.

Some recent work by Mao's group (112–114) have shown that unique SEIs with multilayered structure could be developed and executed on the alkali metal surface by using electrochemical approaches. To be specific, ultrasmooth and ultrathin (USUT) SEI layers for Li and other alkali metals were designed on the basis of the manipulation of electrochemical polishing and follow-up electrolyte reduction (Fig. 3D) (112). The resulting SEI layer could be carefully regulated to manifest alternating inorganic-rich and organic-rich/mixed multilayered structures. The USUT SEI layer on polished LMA, which offers mechanical properties of linked stiffness and elasticity, improved the cycling stability to over 200 cycles at a current density of  $2 \text{ mA cm}^{-2}$ . Furthermore, a variety of single-layered and multilayered SEIs with known compositions and structures can also be fabricated by using the similar electrochemical method (113). The applicability of the method was further demonstrated by using Cu foil as the current collector, and the mechanical properties of these SEIs can be evaluated using AFM nanoindentation. Recently, this research group developed a potentiostatic stripping-galvanostatic plating method to create stable  $\text{LiNO}_3$ -derived multilayer-structured SEI film that successfully suppresses  $\text{NO}_2$  dissolution, Li dendrite formation, and  $\text{O}_2$  corrosion by encapsulating soluble  $\text{NO}_2$  species in the inner area of the SEI (114).

In addition to the electrochemical polishing procedure, in situ electrochemical precharging and electrodeposition techniques have been conducted to build a robust interlayer to safeguard LMAs. For example, an electrochemically activated Li surface with a homogeneous distribution of small pits, which act as preferential nucleation sites during Li plating, can be obtained by including a

short oxidative potentiostatic pulse before the first galvanostatic stripping step in the first cycle (115). Under an inert atmosphere, the simple one-step in situ electrochemical precharging technique has been proven to create thin protective films on LMAs and other-type of electrodes (116). Moreover, Hou *et al.* (117) have proposed an effective strategy to stabilize Li metal by constructing an ex situ SEI film via an electroplating method involving precycling the LMA in an advanced electrolyte. The  $\text{LiF-Li}_3\text{N}$ -enriched SEI is expected to be an electronically insulating film with satisfactory ionic conductivity, which improves the interfacial compatibility and suppresses Li dendrite formation during cell cycling. Gao *et al.* (118) described a nanocomposite layer composed of organic elastomeric salts  $[\text{LiO}-(\text{CH}_2\text{O})_n-\text{Li}]$  and inorganic nanoparticle salts ( $\text{LiF}$ ,  $-\text{NSO}_2-\text{Li}$ , and  $\text{Li}_2\text{O}$ ) that protects the  $\text{Li}_{10}\text{GeP}_2\text{S}_{12}$  (LGPS) SSE and Li metal. Electrochemical decomposition of the liquid electrolyte produces the as-formed nanocomposite layer on Li, which has excellent chemical and electrochemical stability, an affinity for Li and LGPS, and low interfacial resistance.

A special implantable SEI was created using a general electroplating procedure incorporating Li metal precycling in a  $\text{LiTFSI}$  (1.0 M)– $\text{LiNO}_3$  (5.0 wt %)– $\text{Li}_2\text{S}_5$  (0.02 M)–DOL/1,2-dimethoxyethane (DME) ternary salt electrolyte (Fig. 3E) (119). The LMA with the protection of the as-obtained SEI can efficiently match both sulfur and NCM523 cathodes and enhance the electrochemical performance. The excellent high-rate performance of the advanced full cells without any activation confirms the highly conductive properties of electroplated SEIs. In a latest study, Lu *et al.* (120) in situ constructed a stable electrolytic carbon-based hybrid (ECH) artificial SEI on the LMA via electrodeposition of the DME at a high voltage of 700 V. This ECH layer strongly increased the ionic conductivity and mechanical strength, allowing uniform  $\text{Li}^+$  ion diffusion, stabilizing the electrolyte-Li metal contact, and preventing Li dendritic growth and pulverization.

Considering the prospects for mass manufacturing, using as-prepared materials that immediately coat on or interact with Li metal to form an artificial SEI is usually more convenient than electrochemical pretreatment (15). Nevertheless, electrochemical pretreatment methods play a vital role in fundamental investigations, which enable deeper insights into the effects of Li salts, solvents, additives, decomposition products, and electrochemical parameters. This is crucial for a thorough understanding of the composition and structure of the SEI, as well as further electrolyte optimization and interfacial protection.

### Gas-phase pathways

Apart from liquid pretreatment, surface modification with gaseous reagents to create a stable protective layer on LMAs is a desirable choice that provides high accessibility of the reagents to the Li surface and enhances the film uniformity. Therefore, the gas-phase pathway is regarded as an appropriate way to tackle the problems of interfacial issues and volume changes of the LMAs (121, 122).

### Physical vapor deposition

Physical vapor deposition (PVD) is a technique that uses primarily physical means to deposit a thin layer of material. The PVD technique demonstrates special superiority in precisely controlling the components and thickness of the protective layer on LMAs based on

the physical evaporation-deposition principle, when adopted as a primary or secondary manufacturing process.

As a representative PVD method, magnetron sputtering (MS) allows the deposition of metals, alloys, ceramics, and polymer thin films onto Li metal in a vacuum environment to achieve homogeneous protective films with a controllable thickness (121). To build an ion-conducting layer on the Li surface, a silicon layer was fabricated in a radio frequency (RF)-MS system by Tang *et al.* (123). The Si-coated Li foil was heated to 250°C in a glovebox to speed up the alloying between the Li metal and deposited Si to form a  $\text{Li}_x\text{Si}$  layer (Fig. 4A). The  $\text{Li}_x\text{Si}$ -modified LMA shows much more uniform Li dissolution/deposition than the bare LMA. The S and LFP cathodes paired with the  $\text{Li}_x\text{Si}$ -modified LMA showed excellent electrochemical performance in terms of rate capability and cycling stability. A functional ultrathin graphite- $\text{SiO}_2$  bilayered SEI on Li metal fabricated via RF sputtering was demonstrated to facilitate  $\text{Li}^+$  ion diffusion and had higher chemical stability, higher mechanical properties, and lower impedance, which guided a dendrite-free Li deposition (124). A uniform distribution of LiF film on LMAs was realized via the RF-MS process to avoid the side reactions between the LMA and electrolytes (125). As a result, the LiF-coated LMA efficaciously stabilized the interface that enables a uniform Li deposition and longer cycle life.

A scalable sputter process proposed by Cha *et al.* (126) was shown to be able to passivate Li metal from the electrolyte with a 2D  $\text{MoS}_2$  film with the thickness of 10 nm (Fig. 4B). With a large amount of Li atoms intercalating into the unique atomically layered

structure of the  $\text{MoS}_2$ , consistent flow of  $\text{Li}^+$  ions in/out of the LMA is facilitated and the preferential sites for Li dendrite nucleation are eliminated. The symmetric cell of  $\text{MoS}_2$ -coated LMA exhibits low-voltage hysteresis and threefold improvement in cycling performance even at 10  $\text{mA cm}^{-2}$ . Furthermore, in the Li-S full-cell configuration, the use of  $\text{MoS}_2$ -coated LMA results in a specific energy density of  $\sim 589 \text{ Wh kg}^{-1}$  and CE of  $\sim 98\%$  for over 1200 cycles. A similar strategy via the MS deposition of  $\text{MgF}_2$  was also adopted by Li *et al.* (127). The  $\text{MgF}_2$  layer was served as a lithiophilic substrate to form a uniform LiF-Mg dual-layered SEI through its irreversible conversion reaction with Li metal. As a result, the LiF-Mg-coated LMA regulates dendrite-free deposition and provides long-cycle life and high CE in a half-cell. Moreover, Li *et al.* (128) have created a stable and thin  $\text{Cu}_3\text{N}$  layer via the MS technique. The as-prepared  $\text{Cu}_3\text{N}$  can be converted to  $\text{Li}_3\text{N/Cu}$  composite film after Li deposition, working as a highly stable and homogeneous conductive SEI to reduce the formation of Li dendrites in working cells. In addition,  $\text{Li}_3\text{PO}_4$  (129), Sb-doped  $\text{Li}_3\text{PO}_4$  (130), Mg (131), ZnO (132), and amorphous carbon (133) were constructed as protective layers through the MS technique by other research groups, whereby considerable stability improvements in the LMA were also achieved.

Molecular beam epitaxy technique was used to deposit an ultrathin and uniform bismuth (Bi) film on the Li metal surface by thermally evaporating Bi precursor under an ultrahigh vacuum (134). The Bi film is prone to in situ alloying with Li to form a chemically stable alloy interface, which can reduce the harmful side reactions between Li and electrolyte. Moreover, the  $\text{Li}_x\text{Bi}$  alloy-protected

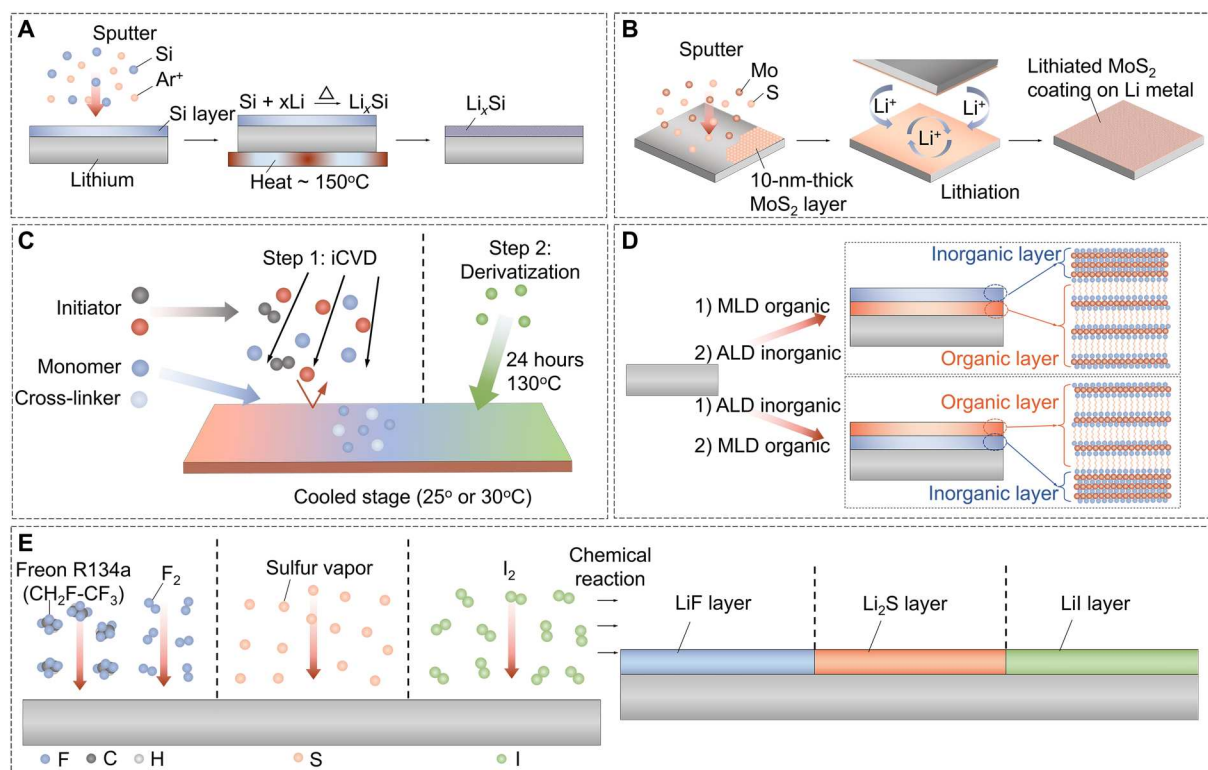


**Fig. 4. Schematic illustration of surface pretreatment using gas-phase pathways.** (A) The preparation process of  $\text{Li}_x\text{Si}$ -modified lithium foil. (B) The fabrication method for a  $\text{MoS}_2$ -coated LMA via sputtering and subsequent lithiation. (C) The fabrication of zwitterionic polymeric interphases. Step 1: iCVD precursor polymer film. Step 2: derivatization. (D) The fabrication process of the dual protective layer by ALD and MLD. (E) The surface processing strategies via chemical reactions with various gases.



LMA offers rapid  $\text{Li}^+$  ion transport and lithiophilic nucleation sites to suppress Li dendrite formation and guide homogeneous Li plating.

### Chemical vapor deposition (CVD)

The CVD method is an advanced synthetic approach for directly growing ultrathin films on electrodes through chemical interactions of precursors at high temperatures (135, 136). Highly uniform and stable protective films on Li metal with atomic-layer thickness can be achieved by this approach.

To rationally design an SEI layer with superior chemical, mechanical, and ion transport properties, Stalin *et al.* (137) used the initiated CVD (iCVD) technique to deposit ultrathin conformal zwitterionic polymeric films as a protective coating on Li metal to stabilize Li electrochemical deposition (Fig. 4C). The molecular structure of zwitterionic moieties at the polymer interface can adjust the solvation environment of the  $\text{Li}^+$  cation, which enables uniform, dendrite-free deposition of Li. As a result, the full cell by pairing a NCM622 cathode with the zwitterionic polymer-coated LMA (negative/positive capacity ratio of 1) exhibits superior capacity retention and stable CE compared to the uncoated LMA. An electron cyclotron resonance CVD apparatus was applied to passivate an LMA with  $\text{Li}_4\text{SiO}_4$ -based thin film (138). The in situ-converted  $\text{Li}_4\text{SiO}_4$  layer efficiently improves  $\text{Li}^+$  ion conductivity and allows dendrite-free Li deposition. Moreover, 2D atomic crystal layers, including hexagonal boron nitride (h-BN) and graphene, can be directly grown on the surface of electrodes via the CVD process (135). The 2D layers afford excellent surface protection of Li metal due to their remarkable mechanical strength, flexibility, and stability. The point and line defects of the 2D layers allow  $\text{Li}^+$  ion infiltration into the electrode, resulting in smooth Li deposition without dendritic and mossy Li formation.

Although CVD is a well-established technique for depositing thin-film coatings, its relatively poor control over the thickness and composition makes it less ideal when applied for the LMA. Atomic layer deposition (ALD) is a self-controlled chemical reaction between gaseous precursors and a solid surface that enables excellent coverage and conformal deposition with rationally designed and precisely controlled composition and thickness (139). For instance, Xie *et al.* (140) demonstrated that LiF can be deposited on the line and point defects of h-BN by ALD. The chemically and mechanically stable LiF/h-BN film efficaciously suppresses Li dendrite formation and improves the CE during extended cycling. With an optimized ALD process, LMAs coated with other ultrathin metal oxide ( $\text{Al}_2\text{O}_3$ ,  $\text{TiO}_2$ , and  $\text{ZrO}_2$ ) layers achieve dendrite-free Li deposition and improved lifetime (141–143). Beyond ALD, molecular layer deposition (MLD) for the LMAs has been further developed by substituting the oxidizing precursor with organic linkers or molecular fragments (144). Pure polymer thin films and organic-inorganic hybrid protective layers can be obtained through the MLD technique. Sun's group (145–148) has demonstrated that various functional protective films can be built on the Li metal by MLD to produce safe high-performance LMBs. For instance, they created an inorganic-organic interlayer (alucone) by MLD at the junction of Li metal and solid-state sulfide electrolytes (145). The interfacial side reactions between Li metal and solid-state sulfide electrolytes are greatly reduced with the aid of the alucone covering layer. In addition, a hybrid polyurea film with controllable components and improved strength was introduced as a protective layer on

Li metal via the MLD process by introducing trimethylaluminum as a cross-linker into the polymer chains (147). A further study by Sun *et al.* (148) reported that a gradient hybrid inorganic-organic polyurea protection film can efficiently enhance the chemical and mechanical properties of the LMAs. The electrically insulating polymer on the coating surface can restrain the volume changes due to its good elasticity, while the inner inorganic lithiophilic sites can helpfully facilitate and regulate uniform Li nucleation and deposition. By combining the ALD and MLD techniques, a hybrid protective film on LMA with precisely controllable structures and robust mechanical properties was constructed (Fig. 4D) (149). The alucone- $\text{Al}_2\text{O}_3$  dual-layer shielded LMA exhibited high stability during the plating/stripping process thus greatly improved cycling performance.

### Chemical reaction with gases

The chemical reaction with a gas to form an artificial SEI on LMAs is an alternate choice that provides high accessibility of reagents to the Li surface and improved film homogeneity. Multitudinous gases (e.g.,  $\text{CH}_2\text{F}-\text{CH}_3$ ,  $\text{F}_2$ , S,  $\text{SeS}_2$ ,  $\text{N}_2$ ,  $\text{I}_2$ , and  $\text{CS}_2$ ) have been conducted to construct a functional protective layer via a spontaneous chemical reaction with metallic Li (122, 150–155). For instance, a conformal and dense LiF layer with controllable thickness coated onto Li metal was developed by exposing Li foil to nonhazardous Freon R134a gas ( $\text{CH}_2\text{F}-\text{CH}_3$ ) (Fig. 4E) (122). The symmetric cells of the layered Li-rGO anodes with the applied LiF layer demonstrated reduced side reactions and highly improved cycling stability without potential polarization augmentation. Furthermore, a homogeneous and compact LiF protective layer on LMAs was developed by a surface fluorination process, which is formed with in situ generated fluorine gas using a fluoropolymer as the precursor (Fig. 4E) (150). The LiF layer shows strong mechanical strength, chemical stability, and low solubility in electrolytes, which can minimize the corrosion reaction between Li metal and organic solvents and suppress Li dendrite formation. As a result, the LiF-coated LMA in symmetric cells enabled a dendrite-free Li deposition and stable cycling over 300 cycles in carbonate electrolytes. Lin *et al.* (152) reported a solid-gas reaction method to fabricate a dense LiI protective layer on the LMA surface by using a Li metal reaction with iodine vapor (Fig. 4E). In addition, a special "sauna" reaction between  $\text{CS}_2$ - $\text{I}_2$  mixed steam and Li metal was conducted to form a SEI layer with high mechanical property and high ionic conductivity, which consists of amorphous carbon and Li compounds ( $\text{Li}_2\text{S}$  and LiI) (153). The obtained C- $\text{Li}_2\text{S}$ -LiI@Li anode exhibits outstanding electrochemical performance with low-voltage polarization and long-cycle life.

Apart from the lithium halides, lithium chalcogenides with high ionic conductivity are also attractive. Chen *et al.* (154) reported that a homogenous  $\text{Li}_2\text{S}$  protective layer can be fabricated by reacting Li with sulfur vapor at an elevated temperature (Fig. 4E). Specifically, the uniform  $\text{Li}_2\text{S}$ -based protective layer turned into a layered SEI that preserves protective function with high ionic conductivity, rather than into a disordered, broken SEI mainly composed of parasitic reaction products. Similarly, Liu *et al.* (155) proposed a gas-solid reaction to fabricate a stable  $\text{Li}_2\text{S}/\text{Li}_2\text{Se}$  mixed SEI via the reaction between  $\text{SeS}_2$  gas and Li metal at a low temperature. The migration barrier energy of  $\text{Li}_2\text{Se}$  is lower than that of  $\text{Li}_2\text{S}$  at different lattice planes, thus confirming the positive function of  $\text{Li}_2\text{Se}$  in improving the integral ionic conductivity.

$\text{Li}_3\text{N}$  shows high ionic conductivity (up to  $10^{-3} \text{ S cm}^{-1}$ ) and low electronic conductivity ( $<10^{-12} \text{ S cm}^{-1}$ ), which is suitable for Li metal protection. A pinhole-free and ionically conductive  $\alpha\text{-Li}_3\text{N}$  layer was prepared on the surface of Li metal by directly reacting clean molten Li foil with pure nitrogen gas at  $450^\circ\text{C}$  in the argon atmosphere (151). This  $\text{Li}_3\text{N}$  layer is chemically stable, which can isolate the reactive Li metal from the organic solvent, prevent continuous electrolyte consumption during cycling, and suppress Li dendrite growth in the Li plating/stripping process.

### Other peculiar pathways

The plasma state is frequently referred to the fourth state of matter in the sequence: solid, liquid, gas, and plasma (156). In general, plasma is made up of extremely reactive electrons, ions, and neutral species that are created by high-voltage ionization (157). Through energy exchange, plasma reagents may quickly produce a large number of active sites on the material surface, allowing reactions with high barriers to proceed under mild circumstances in a matter of minutes (158). Therefore, plasma treatment appears to be a promising method for high-quality surface engineering of LMAs. For example, Chen *et al.* (159) obtained a  $\text{Li}_3\text{N}$  protective layer with high modulus and high ionic conductivity on LMAs by a plasma activation of Li metal in a  $\text{N}_2$  environment (Fig. 5A). This desired  $\text{Li}_3\text{N}$  protective layer can efficiently prevent spontaneous reactions between the highly reactive Li metal and the organic electrolyte and suppress dendritic Li generation during the Li plating/stripping

process. Recently, Cao *et al.* (160) used a rapid  $\text{CF}_4$  plasma treatment process to construct an artificial SEI consisting of  $\text{LiF}$  and  $\text{Li}_2\text{C}_2$  on LMAs via ion bombardment. Benefiting from the high adsorption energy, low diffusion barrier, and high mechanical strength of the  $\text{LiF}$  and  $\text{Li}_2\text{C}_2$  components, the obtained composite layer guaranteed a stable interface and dendrite-free Li deposition after long cycling. Moreover, the room-temperature plasma treatment described in these works is highly tunable and environmentally friendly and has potential in large-scale energy storage applications.

Some interesting and uncommon strategies beyond the above pathways, such as combining the different methods to construct multiple protective layers (161), the concepts of "solid-liquid membrane" (162), "spansule" (163), and "self-assembled monolayer" (164), have been proposed for creating various artificial SEIs on the LMAs. For example, Liu *et al.* proposed that a dynamically cross-linked polymer (silly putty) manifested a "solid-liquid" hybrid behavior, which enabled it to act as an adaptive interlayer for LMAs (Fig. 5B) (162). In response to the Li growth rate, the dynamic polymer can reversibly switch between "liquid" and "solid" qualities to support uniform coverage and prohibit Li dendrite formation, allowing reliable operation of LMAs. In addition, Yuan *et al.* (163) designed a smart "spansule" made of carbon-coated mixed metal fluoride ( $\text{NMMF@C}$ ) core@shell microstructures to provide a long-lasting supply of functional ingredients for stabilizing LMAs (Fig. 5C). With the assistance of cryo-TEM, they found that the NMMF core would gradually dissolve and release functional metal and fluoride ions into the electrolyte during cycling, while the in situ-formed metal layer and  $\text{LiF}$ -involved bilayer interface would be beneficial for guiding uniform Li deposition. Consequently, a high CE of approximately 98% is achieved for over 1000 cycles at a current density of  $2 \text{ mA cm}^{-2}$  with a capacity of  $1 \text{ mAh cm}^{-2}$ . To precisely construct a passive SEI to enable stable LMAs at low temperatures, Gao *et al.* (164) fabricated a self-assembled electrochemically active monolayer on the Cu current collector, which can regulate the nanostructure and component of the SEI and deposition behavior of Li metal (Fig. 5D). The as-formed SEI contains a  $\text{LiF}$ -rich inner phase and an amorphous outer layer that effectively sealed the Li surface. As a result, galvanic Li corrosion and self-discharge were suppressed, dendrite-free Li deposition was achieved from  $-60^\circ$  to  $45^\circ\text{C}$ , and the LMB ( $\text{Li}/\text{LiCoO}_2$  cells) exhibits 200-cycle life span at  $-15^\circ\text{C}$  with a recharge time of 45 min.

### CHARACTERIZATION TECHNIQUES

Since the surface of LMAs has been precisely modified using various surface engineering strategies, direct investigation of the physical and chemical properties of these protective layers is vitally important to understand the electrochemical behavior of LMAs. The following scientific issues are the major concerns during the surface investigation of LMAs: (i) the morphology, particle size, and thickness of the layers; (ii) the chemical composition, elemental content, and chemical state; (iii) the stiffness and elastic modulus; and (iv) the structural evolution at multiple spatial scales. Characterization tools play a key role in understanding these scientific issues, include x-ray diffraction (XRD), x-ray photoelectron spectroscopy (XPS), Fourier transform infrared (FTIR) spectroscopy, Raman spectroscopy, solid-state nuclear magnetic resonance (NMR), time-of-

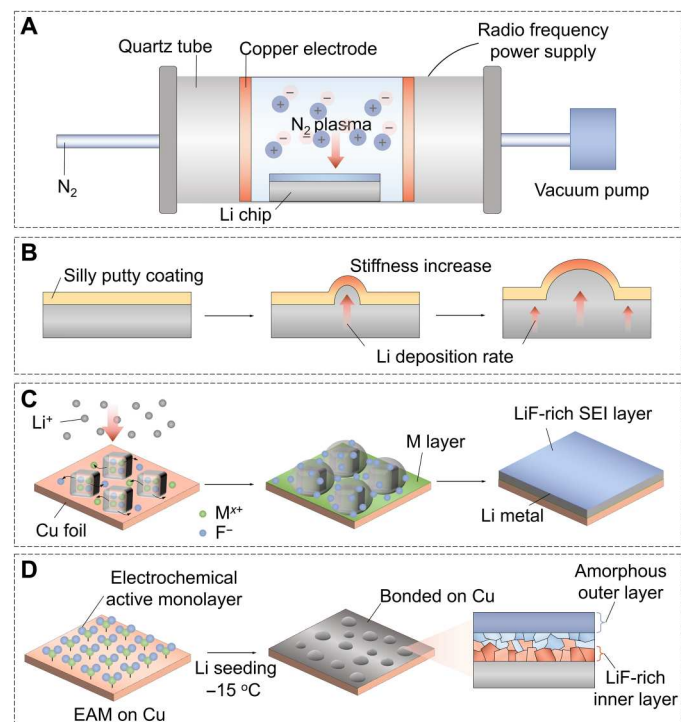


**Fig. 5. Schematic illustration of surface pretreatment using some peculiar pathways.** (A) A desired  $\text{Li}_3\text{N}$  film can be formed on the Li metal as the protective layer by a plasma activation in a short time. (B) The design of silly putty modified LMA. (C) A designed "spansule" can sustainably supply functional ingredients that effectively guide dendrite-free Li deposition. (D) A self-assembled monolayer of electrochemically active 1,3-benzenedisulfonyl fluoride on Cu can lead to uniform seeding of Li with a stable  $\text{LiF}$ -rich SEI layer.

flight secondary ion mass spectrometry (TOF-SIMS), optical microscopy (OM), scanning electron microscopy (SEM), AFM, TEM, cryo-TEM, and several other advanced methods. All these techniques can be categorized in terms of the study of composition or morphology (Fig. 6).

### Composition

XRD is one of the well-established techniques to study the crystal structure and structural changes of surficial materials before and after reactions on LMAs. According to the peak positions and relative intensities, information about the crystal structure, phase purity, and structural evolution of various inorganic components within the protective layers can be obtained, such as Li-based alloys ( $\text{Li}_x\text{M}$ ) and compounds (i.e.,  $\text{LiF}$ ,  $\text{Li}_3\text{N}$ ,  $\text{LiCl}$ ,  $\text{Li}_2\text{S}$ ,  $\text{Li}_x\text{PO}_4$ , etc.) (165).

XPS is the most extensively used analytical technique for surface analysis, providing element-specific composition and electronic state information (166). As a powerful quantitative technique, XPS has several merits as follows: (i) sensitivity to all the elements with the same order of magnitude; (ii) easy observation of the chemical shift information; (iii) ability to identify elements half-

quantitatively; (iv) sensitivity for surface analysis with an ultrathin depth (2 to 5 nm). Theoretically, the electronic states of cations and anions in the entire artificial SEI can be expediently obtained by XPS analysis. Moreover, XPS can probe the change in the chemical state of elements in the protective layer after Li plating or cycling.

FTIR spectroscopy is not only a surface sensitive but also a non-destructive technique for acquiring accurate information about characteristic functional groups within the protective layers on the LMAs. It is especially suitable for investigating the organic species, which can complement the composition information from XRD and XPS. For qualitative analysis, FTIR spectroscopy has the advantages of short data collection time, small sample size requirement, and simple data collection procedure (167). Although the FTIR helps detect surface components, it only identifies dipole moment changes. Raman spectroscopy measures the inelastic scattering induced by polarizability changes, and it is especially helpful for analyzing carbon-based materials, such as graphene, GO, rGO, and their derivatives (168). Therefore, Raman and FTIR spectroscopies are complementary techniques in most circumstances of surface investigation.

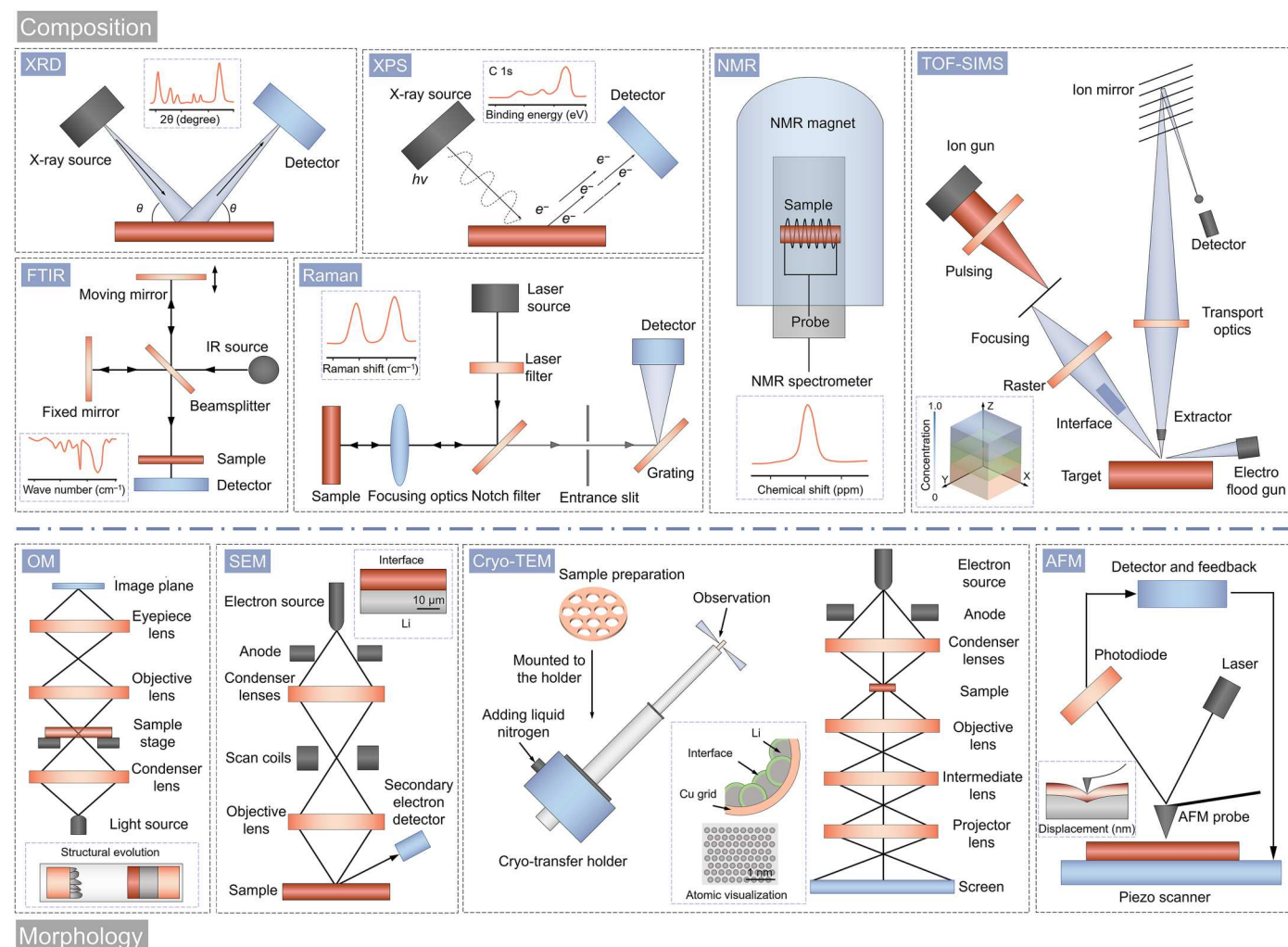


**Fig. 6. Schematic illustration of the current characterization techniques for the artificial SEIs on Li metal.**



Solid-state NMR spectroscopy is another important analytical technique to probe the local structural environments and electronic structure of surface materials for LMAs. A variety of precise structural details about the materials can be revealed based on the peak chemical shift, peak shape, and coupling constant of the nucleus (167). Therefore, many researchers have used the solid-state NMR to identify the organic components in the SEI of LMAs, which could assist to reveal their molecular structures and disclose the characteristics of Li-ion transport between SEI and the deposited Li (169).

TOF-SIMS is a material characterization technique with strong chemical sensitivity, high surface sensitivity (upper 2 to 3 nm probed), and molecular specificity (170). The depth profiling can identify species of the SEI and their 3D distribution on the micro- to the nanometer scale, which could be combined with atom probe tomography to show the chemistry and distribution of the SEI on the atomic scale. For example, Sun's group (146–149) performed TOF-SIMS to identify the distribution and depth profiles of various molecular moieties within the artificial SEIs coated on LMAs, such as polyurea, zirconium film,  $\text{Al}_2\text{O}_3$ , and alucone dual layer.

### Morphology

OM observations can provide a direct imaging of structural evolution of the protective layers during the vertical growth and dissolution of Li metals in electrolytes but are limited at micron-level magnification (171). SEM has been mainly used for the observation of microstructures and thicknesses of the protective layers. However, traditional SEM has been confined to 2D information and relatively low resolutions. Advanced imaging techniques, including TEM and scanning TEM (STEM), operate at a high acceleration voltage, enabling highly enlarged orthographic images to be achieved with exceptional spatial resolution down to the atomic scale (25). In this regard, TEM and STEM are critical techniques for examining the morphological structure and thin layer on the Li surface. Combination of microscopic and spectroscopic techniques, such as SEM/TEM–energy-dispersive spectroscopy and STEM–electron energy loss spectroscopy, enables the multiangle investigation of not only the morphology but also the structure, local elemental distribution, chemical information, and bonding environment correlated to the local electrode materials simultaneously.

Nevertheless, the high-energy electron beams can permanently destroy the SEI layer and Li metal due to their weak atomic bonding and relatively low melting point. Therefore, observing the original morphology and chemical components of the SEI layer seems difficult. To discover more reliable characterization methods for SEI layers, scientists paid particular attention to cryo-TEM, which is mainly used for the characterization of biological materials. Cryo-TEM is thought to be capable of preserving the initial structure and morphology of materials at extremely low temperatures (172). Specifically, Cui's group (173) has pioneered to use the cryo-TEM to investigate the atomic structure of SEI films formed on the surface of Li metal in different electrolyte. Motivated from the excellent effectiveness of the cryo-TEM for LMAs, more researchers have revealed the structure of the SEIs and their evolution behaviors (42, 110, 174–176). By using the cryo-TEM technique, a relationship between the SEI nanostructures and electrochemical properties may be established.

AFM is a type of microscopy that scans the surface of the sample and records the van der Waals force that exists between the probe

and sample. It can measure the overall surface structure, height distribution, and roughness of the Li surface. Therefore, primary quality assessments of SEIs can be performed using the AFM technique to examine their morphological characteristics and mechanical properties (169). In particular, the nanoindentation characteristics, which are revealed by force probing in areas where surface deformation occurs, reveal the fine mechanical properties of SEIs that are governed by the chemical compositions and spatial arrangements, and they may be used to assess the SEI quality. For example, Mao's group (113) used a set of unique nanoindentation features of mechanical properties as standards for evaluating the quality of unknown SEIs, including Young's modulus, thickness, and smoothness.

### CONCLUSION AND PERSPECTIVE

Surface engineering has been developed to address the critical application issues of LMAs for nearly three decades since its first demonstration in 1993 reported by Takehara *et al.* (72). However, this realm was developed slowly in the following two decades, which focused mainly on the liquid phase–dominated pathways. In 2014, Zheng *et al.* (18) first reported a solid phase–involved surface engineering approach, in which a protective layer assembled by free-standing interconnected hollow carbon nanospheres was built on the LMAs. Since then, research on the development of various surface engineering strategies is booming, including treating the Li metal toward the reagents under the states of matter beyond the solid or liquid (gas and plasma for instance) and using some unique pathways. The roadmap of this realm is illustrated in Fig. 7A. The cycling performance of the modified LMAs fabricated via different surface engineering strategies and the evaluation of these strategies from five practical application metrics are summarized in Fig. 7 (B to D). The LMAs pretreated by the solid-phase strategy have better cycling performance in ether-based electrolytes than those in carbonate-based ones, among which the method of membrane modification is the best (Fig. 7B). However, the disadvantage of using the solid-phase strategy is that the artificial SEI is usually thick (larger than 10  $\mu\text{m}$  and up to 160  $\mu\text{m}$  in thickness), resulting in a relatively small-volume energy density for practical application. Still, the solid-phase strategy scores well on the metrics of protection efficiency, cost effectiveness, and processing simplicity. Similar to the solid-phase strategy, the LMAs pretreated by the liquid-phase one also show better stability in the ether-based electrolyte, and the three representative methods are rivals in the cycling performance (Fig. 7C). In terms of the practical application, the “solution casting” and “chemical reaction with liquids” score well in all the five metrics, while the “electrochemical treatment” has only one comparative advantage in constructing thin artificial SEIs, which make it leading in the metrics of volume energy density. Compared with the previous two strategies, the cycling performance of the LMAs pretreated by the gas-phase one is generally mediocre, which might be due to that the electrolytes used are all carbonates (Fig. 7D). The cycling performance of these LMAs in ether-based electrolytes needs to be investigated. It is worth mentioning that the gas-phase strategy has a prominent merit for constructing ultrathin artificial SEIs, whose thickness can be as small as less than 10 nm, so its score for the “volume energy density” is the highest. However, as the equipment used in the gas-phase strategy is

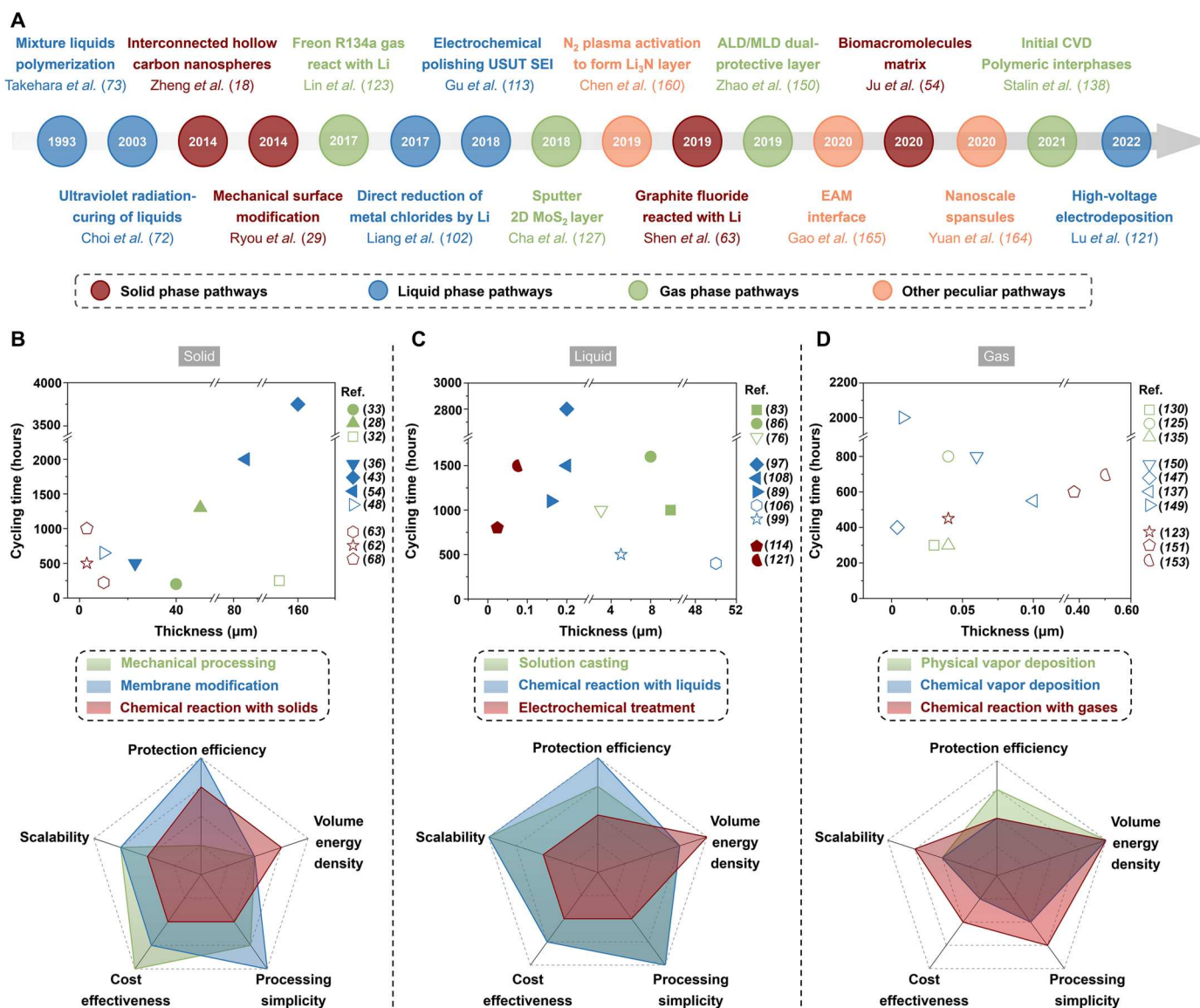


**Fig. 7. Summary and comparison of various surface pretreatment strategies for LMAs.** (A) Roadmap of major achievements in the field of surface engineering. (B to D) The panels on the upper row are the cycling performance of Li symmetric cell (current density and capacity is 1 mA cm<sup>-2</sup> and 1 mAh cm<sup>-2</sup>, respectively) using the modified LMAs pretreated by different methods. The solid symbols represent using the ether-based electrolytes, while the hollow ones mean using the carbonate-based electrolytes. The panels on the nether row are the evaluation of these methods from five practical application metrics: protective efficiency, volume energy density, processing simplicity, cost effectiveness, and scalability.

usually expensive, it is less cost-effective, while the other three metrics are moderate.

Although fruitful achievements have been achieved in the surface engineering for stabilizing the LMAs, many challenges still need to be considered: (i) The artificial SEIs constructed by current surface pretreatment techniques are still far from satisfactory for the LMAs. For example, the majority of the documented artificial SEIs are restricted to a single ingredient, which is insufficient to meet the longevity and safety requirements of LMAs. To create SEIs with multi-ingredient to realize the maximum of their functionality, combining multiple strategies is therefore worthwhile (161). Besides, potential new methods are always welcome to be explored, such as liquid phase-based SEI production assisted by

speedy and accurate laser-mediated technology or solid phase-based patterned SEI constructed by 3D printing. (ii) The relationship between the structure of the artificial SEIs and battery performance is still not clear. Thus, more precise construction of the SEI's components and thicknesses by advanced surface engineering protocols, for example, an affordable CVD-based technology, is needed. Accordingly, a selection rule for a specific component and its proper spatial and temporal distribution in the artificial SEIs can be established for an oriented preparation by surface engineering. (iii) Implementing surface engineering for practical applications in LMAs is still challenging. For instance, it is necessary to make the transition of the surface engineering from coin cells to pouch cells feasible for mass manufacturing. Furthermore,

exploiting novel surface engineering strategies to build stable artificial SEIs that can work under certain challenging circumstances, such as low negative/positive capacity ratio, lean electrolytes, high current densities, and extreme temperature, should be put on the schedule. Last but not the least, more metrics must be considered for the evaluation of the practicality of the surface engineering processes (such as toxicity and environmental compatibility).

This review has also provided a concise summary of the current developments in the key characterization techniques used to examine the composition and structure of the artificial SEIs on the LMAs. However, these characterization techniques still have some limitations: (i) XRD has difficulty in obtaining detailed information on amorphous materials and organic components. (ii) It is challenging for XPS to provide deep-layer information. Also, the XPS etching procedure carries the risk of radiation damage, chemical-state changes brought by low-energy electrons, or sample contamination. (iii) Normal FTIR and Raman spectra have a relatively low spatial resolution due to the Abbe diffraction limit. (iv) The relatively low sensitivity and resolution of solid-state NMR poses challenges for studying the artificial SEIs. (v) The TOF-SIMS equipment is expensive and not readily available, while the sample testing process is also inconvenient. (vi) The SEI and Li metal will inevitably be irreversibly damaged by high-energy electron beams using SEM and TEM techniques. (vii) The AFM has strict criteria for the sample surface flatness. Therefore, a combination of diverse microscopic and spectroscopic techniques would be desirable, which enables simultaneous multi-angle analysis of the morphology, structure, elemental composition, and coordination chemistry of the electrode interface. For example, recent developments in combining light-induced molecular excitations with mechanical force detection are particularly interesting since they aim to improve the chemical selectivity of AFM (177). Nano-IR, which has been used effectively to visualize molecular layers on surfaces with chemical selectivity and with a spatial resolution as low as 25 nm (178), is a potentially powerful tool for this field. It should also be emphasized that the inherent sensitivity of Li metal and its SEI to air makes it difficult to transfer the samples to the instrument. Hence, how to achieve damage-free transfer and characterization is a challenge. On the one hand, researchers could interconnect these instruments with the glovebox via ducted vacuum for simultaneous characterization of the sample at the same location, as well as avoid potential contamination during the sample transfer. In addition, some non-destructive imaging techniques could be used, such as low-dose TEM imaging and x-ray computed tomography. On the other hand, more efforts need to be devoted to advance in situ/operando characterization tools, which can deliver more trustworthy and precise information by continually monitoring the evolution of the target materials and the intricate physical and chemical processes during the cycling, for example, the degradation mechanism of the artificial SEIs (169, 170).

In conjunction with interdisciplinary research (including chemical engineering, materials, nanotechnology, physics, chemistry, electrochemistry, etc.), more reliable artificial SEIs on LMAs can be rationally designed by advanced surface engineering. After more researchers joining in this fast-growing field with persistent cooperation and dedication, it is believed that many exciting discoveries on surface engineering can be expected in the years ahead, which will drive a greater breakthrough of the LMAs and other energy storage systems.

## REFERENCES AND NOTES

1. X. B. Cheng, R. Zhang, C. Z. Zhao, Q. Zhang, Toward safe lithium metal anode in rechargeable batteries: A review. *Chem. Rev.* **117**, 10403–10473 (2017).
2. X. Zhang, Y. Yang, Z. Zhou, Towards practical lithium-metal anodes. *Chem. Soc. Rev.* **49**, 3040–3071 (2020).
3. D. Lin, Y. Liu, Y. Cui, Reviving the lithium metal anode for high-energy batteries. *Nat. Nanotechnol.* **12**, 194–206 (2017).
4. W. Xu, J. Wang, F. Ding, X. Chen, E. Nasybulin, Y. Zhang, J.-G. Zhang, Lithium metal anodes for rechargeable batteries. *Energ. Environ. Sci.* **7**, 513–537 (2014).
5. X. Zhang, A. Wang, X. Liu, J. Luo, Dendrites in lithium metal anodes: Suppression, regulation, and elimination. *Acc. Chem. Res.* **52**, 3223–3232 (2019).
6. T. Li, X.-Q. Zhang, P. Shi, Q. Zhang, Fluorinated solid-electrolyte interphase in high-voltage lithium metal batteries. *Joule* **3**, 2647–2661 (2019).
7. W. Liu, P. Liu, D. Mitlin, Review of emerging concepts in SEI analysis and artificial SEI membranes for lithium, sodium, and potassium metal battery anodes. *Adv. Energy Mater.* **10**, 2002297 (2020).
8. H. Wang, D. Yu, C. Kuang, L. Cheng, W. Li, X. Feng, Z. Zhang, X. Zhang, Y. Zhang, Alkali metal anodes for rechargeable batteries. *Chem* **5**, 313–338 (2019).
9. J. W. Choi, D. Aurbach, Promise and reality of post-lithium-ion batteries with high energy densities. *Nat. Rev. Mater.* **1**, 16013 (2016).
10. S. Wei, S. Choudhury, Z. Tu, K. Zhang, L. A. Archer, Electrochemical interphases for high-energy storage using reactive metal anodes. *Acc. Chem. Res.* **51**, 80–88 (2018).
11. C. B. Jin, T. F. Liu, O. W. Sheng, M. Li, W. K. Zhang, J. W. Nai, Z. J. Ju, Y. J. Liu, T. C. Liu, Y. Wang, Y. F. Yuan, Z. Lin, J. Lu, X. Y. Tao, Rejuvenating dead lithium supply in lithium metal anodes by iodine redox. *Nat. Energy* **6**, 378–387 (2021).
12. F. Liu, R. Xu, Y. Wu, D. T. Boyle, A. Yang, J. Xu, Y. Zhu, Y. Ye, Z. Yu, Z. Zhang, X. Xiao, W. Huang, H. Wang, H. Chen, Y. Cui, Dynamic spatial progression of isolated lithium during battery operations. *Nature* **600**, 659–663 (2021).
13. P. C. Zou, Y. Sui, H. Zhan, C. Wang, H. L. Xin, H. M. Cheng, F. Kang, C. Yang, Polymorph evolution mechanisms and regulation strategies of lithium metal anode under multi-physical fields. *Chem. Rev.* **121**, 5986–6056 (2021).
14. Y. J. Liu, X. Y. Tao, Y. Wang, C. Jiang, C. Ma, O. W. Sheng, G. X. Lu, X. W. Lou, Self-assembled monolayers direct a LiF-rich interphase toward long-life lithium metal batteries. *Science* **375**, 739–745 (2022).
15. X.-Q. Zhang, X.-B. Cheng, Q. Zhang, Advances in interfaces between Li metal anode and electrolyte. *Adv. Mater. Inter.* **5**, 1701097 (2018).
16. R. Xu, X.-B. Cheng, C. Yan, X.-Q. Zhang, Y. Xiao, C.-Z. Zhao, J.-Q. Huang, Q. Zhang, Artificial interphases for highly stable lithium metal anode. *Matter* **1**, 317–344 (2019).
17. M. D. Tikekar, S. Choudhury, Z. Tu, L. A. Archer, Design principles for electrolytes and interfaces for stable lithium-metal batteries. *Nat. Energy* **1**, 16114 (2016).
18. G. Y. Zheng, S. W. Lee, Z. Liang, H. W. Lee, K. Yan, H. Yao, H. Wang, W. Li, S. Chu, Y. Cui, Interconnected hollow carbon nanospheres for stable lithium metal anodes. *Nat. Nanotechnol.* **9**, 618–623 (2014).
19. Y. C. Yin, Q. Wang, J. T. Yang, F. Li, G. Zhang, C. H. Jiang, H. S. Mo, J. S. Yao, K. H. Wang, F. Zhou, H. X. Ju, H. B. Yao, Metal chloride perovskite thin film based interfacial layer for shielding lithium metal from liquid electrolyte. *Nat. Commun.* **11**, 1761 (2020).
20. H. Wu, H. Jia, C. Wang, J.-G. Zhang, W. Xu, Recent progress in understanding solid electrolyte interphase on lithium metal anodes. *Adv. Energy Mater.* **11**, 2003092 (2021).
21. S. Gao, F. Sun, N. Liu, H. Yang, P.-F. Cao, Ionic conductive polymers as artificial solid electrolyte interphase films in Li metal batteries - A review. *Mater. Today* **40**, 140–159 (2020).
22. Q. Zhang, S. Liu, Y. Lu, L. Xing, W. Li, Artificial interphases enable dendrite-free Li-metal anodes. *J. Energy Chem.* **58**, 198–206 (2021).
23. M. Du, K. Liao, Q. Lu, Z. Shao, Recent advances in the interface engineering of solid-state Li-ion batteries with artificial buffer layers: Challenges, materials, construction, and characterization. *Energ. Environ. Sci.* **12**, 1780–1804 (2019).
24. Z. Wang, Y. Wang, C. Wu, W. K. Pang, J. Mao, Z. Guo, Constructing nitrated interfaces for stabilizing Li metal electrodes in liquid electrolytes. *Chem. Sci.* **12**, 8945–8966 (2021).
25. J. Tan, J. Matz, P. Dong, J. Shen, M. Ye, A growing appreciation for the role of LiF in the solid electrolyte interphase. *Adv. Energy Mater.* **11**, 2100046 (2021).
26. R. G. Fedorov, S. Maletti, C. Heubner, A. Michaelis, Y. Ein-Eli, Molecular engineering approaches to fabricate artificial solid-electrolyte interphases on anodes for Li-ion batteries: A critical review. *Adv. Energy Mater.* **11**, 2101173 (2021).
27. Y.-J. Kim, H. S. Jin, D.-H. Lee, J. Choi, W. Jo, H. Noh, J. Lee, H. Chu, H. Kwack, F. Ye, H. Lee, M.-H. Ryou, H.-T. Kim, Guided lithium deposition by surface micro-patterning of lithium-metal electrodes. *ChemElectroChem* **5**, 3169–3175 (2018).
28. H. Wang, P. Hu, X. Liu, Y. Shen, L. Yuan, Z. Li, Y. Huang, Sowing silver seeds within patterned ditches for dendrite-free lithium metal batteries. *Adv. Sci.* **8**, 2100684 (2021).



29. M.-H. Ryou, Y. M. Lee, Y. Lee, M. Winter, P. Bieker, Mechanical surface modification of lithium metal: Towards improved Li metal anode performance by directed Li plating. *Adv. Funct. Mater.* **25**, 834–841 (2014).
30. J. Park, J. Jeong, Y. Lee, M. Oh, M.-H. Ryou, Y. M. Lee, Micro-patterned lithium metal anodes with suppressed dendrite formation for post lithium-ion batteries. *Adv. Mater. Inter.* **3**, 1600140 (2016).
31. Q. Li, B. Quan, W. Li, J. Lu, J. Zheng, X. Yu, J. Li, H. Li, Electro-plating and stripping behavior on lithium metal electrode with ordered three-dimensional structure. *Nano Energy* **45**, 463–470 (2018).
32. H. Kim, Y. J. Gong, J. Yoo, Y. S. Kim, Highly stable lithium metal battery with an applied three-dimensional mesh structure interlayer. *J. Mater. Chem. A* **6**, 15540–15545 (2018).
33. D. Wang, C. Luan, W. Zhang, X. Liu, L. Sun, Q. Liang, T. Qin, Z. Zhao, Y. Zhou, P. Wang, W. Zheng, Zipper-inspired SEI film for remarkably enhancing the stability of Li metal anode via nucleation barriers controlled weaving of lithium pits. *Adv. Energy Mater.* **8**, 1800650 (2018).
34. D. Liebenau, K. Jalkanen, S. Schmohl, M. C. Stan, P. Bieker, H.-D. Wiemhöfer, M. Winter, M. Kolk, Improved interfaces of mechanically modified lithium electrodes with solid polymer electrolytes. *Adv. Mater. Inter.* **6**, 1900518 (2019).
35. M. S. Kim, J.-H. Ryu, Deepika, Y. R. Lim, I. W. Nah, K.-R. Lee, L. A. Archer, W. I. Cho, Langmuir-blodgett artificial solid-electrolyte interphases for practical lithium metal batteries. *Nat. Energy* **3**, 889–898 (2018).
36. N. Li, K. Zhang, K. Xie, W. Wei, Y. Gao, M. Bai, Y. Gao, Q. Hou, C. Shen, Z. Xia, B. Wei, Reduced-graphene-oxide-guided directional growth of planar lithium layers. *Adv. Mater.* **32**, 1907079 (2020).
37. X. B. Cheng, T. Z. Hou, R. Zhang, H. J. Peng, C. Z. Zhao, J. Q. Huang, Q. Zhang, Dendrite-free lithium deposition induced by uniformly distributed lithium ions for efficient lithium metal batteries. *Adv. Mater.* **28**, 2888, 2895 (2016).
38. P. Zhai, T. Wang, H. Jiang, J. Wan, Y. Wei, L. Wang, W. Liu, Q. Chen, W. Yang, Y. Cui, Y. Gong, 3D artificial solid-electrolyte interphase for lithium metal anodes enabled by insulator-metal-insulator layered heterostructures. *Adv. Mater.* **33**, 2006247 (2021).
39. C. Sun, A. Lin, W. Li, J. Jin, Y. Sun, J. Yang, Z. Wen, In situ conversion of  $\text{Cu}_3\text{P}$  nanowires to mixed ion/electron-conducting skeleton for homogeneous lithium deposition. *Adv. Energy Mater.* **10**, 1902989 (2019).
40. K. Xie, K. Yuan, K. Zhang, C. Shen, W. Lv, X. Liu, J. G. Wang, B. Wei, Dual functionalities of carbon nanotube films for dendrite-free and high energy-high power lithium-sulfur batteries. *ACS Appl. Mater. Inter.* **9**, 4605–4613 (2017).
41. Y. Ma, P. Qi, J. Ma, L. Wei, L. Zhao, J. Cheng, Y. Su, Y. Gu, Y. Lian, Y. Peng, Y. Shen, L. Chen, Z. Deng, Z. Liu, Wax-transferred hydrophobic CVD graphene enables water-resistant and dendrite-free lithium anode toward long cycle Li-air battery. *Adv. Sci.* **8**, 2100488 (2021).
42. B. Han, D. Feng, S. Li, Z. Zhang, Y. Zou, M. Gu, H. Meng, C. Wang, K. Xu, Y. Zhao, H. Zeng, C. Wang, Y. Deng, Self-regulated phenomenon of inorganic artificial solid electrolyte interphase for lithium metal batteries. *Nano Lett.* **20**, 4029–4037 (2020).
43. Z. J. Ju, C. B. Jin, H. D. Yuan, T. Yang, O. W. Sheng, T. F. Liu, Y. J. Liu, Y. Wang, F. Y. Ma, W. K. Zhang, J. W. Nai, X. Y. Tao, A fast-ion conducting interface enabled by aluminum silicate fibers for stable Li metal batteries. *Chem. Eng. J.* **408**, 128016 (2021).
44. K. Lu, S. Gao, R. J. Dick, Z. Sattar, Y. Cheng, A fast and stable Li metal anode incorporating an  $\text{Mo}_6\text{S}_8$  artificial interphase with super Li-ion conductivity. *J. Mater. Chem. A* **7**, 6038–6044 (2019).
45. N. Li, W. Wei, K. Xie, J. Tan, L. Zhang, X. Luo, K. Yuan, Q. Song, H. Li, C. Shen, E. M. Ryan, L. Liu, B. Wei, Suppressing dendritic lithium formation using porous media in lithium metal-based batteries. *Nano Lett.* **18**, 2067–2073 (2018).
46. B. Zhu, Y. Jin, X. Hu, Q. Zheng, S. Zhang, Q. Wang, J. Zhu, Poly(dimethylsiloxane) thin film as a stable interfacial layer for high-performance lithium-metal battery anodes. *Adv. Mater.* **29**, 1603755 (2017).
47. G. Y. Zheng, C. Wang, A. Pei, J. Lopez, F. Shi, Z. Chen, A. D. Sendek, H.-W. Lee, Z. Lu, H. Schneider, M. M. Safont-Sempere, S. Chu, Z. Bao, Y. Cui, High-performance lithium metal negative electrode with a soft and flowable polymer coating. *ACS Energy Lett.* **1**, 1247–1255 (2016).
48. R. M. Gao, H. Yang, C. Y. Wang, H. Ye, F. F. Cao, Z. P. Guo, Fatigue-resistant interfacial layer for safe lithium metal batteries. *Angew. Chem. Int. Ed.* **60**, 25508 (2021).
49. Z. Zhang, Z. Peng, J. Zheng, S. Wang, Z. Liu, Y. Bi, Y. Chen, G. Wu, H. Li, P. Cui, Z. Wen, D. Wang, The long life-span of a Li-metal anode enabled by a protective layer based on the pyrolyzed N-doped binder network. *J. Mater. Chem. A* **5**, 9339–9349 (2017).
50. W. Fan, R. Zhang, Z. Wang, X. Lei, C. Qin, X. Liu, Facile fabrication of polyether sulfone (PES) protecting layer on Cu foil for stable Li metal anode. *Electrochim. Acta* **260**, 407–412 (2018).
51. H. Liu, R. Tao, C. Guo, W. Zhang, X. Liu, P. Guo, T. Zhang, J. Liang, Lithiated halloysite nanotube/cross-linked network polymer composite artificial solid electrolyte interface layer for high-performance lithium metal batteries. *Chem. Eng. J.* **429**, 132239 (2022).
52. T. Wang, Y. Li, J. Zhang, K. Yan, P. Jaumaux, J. Yang, C. Wang, D. Shanmukaraj, B. Sun, M. Armand, Y. Cui, G. Wang, Immunizing lithium metal anodes against dendrite growth using protein molecules to achieve high energy batteries. *Nat. Commun.* **11**, 5429 (2020).
53. L. B. Mao, H. L. Gao, H. B. Yao, L. Liu, H. Colfen, G. Liu, S. M. Chen, S. K. Li, Y. X. Yan, Y. Y. Liu, S. H. Yu, Synthetic nacre by predesigned matrix-directed mineralization. *Science* **354**, 107–110 (2016).
54. Z. J. Ju, J. W. Nai, Y. Wang, T. F. Liu, J. H. Zheng, H. D. Yuan, O. W. Sheng, C. B. Jin, W. K. Zhang, Z. Jin, H. Tian, Y. J. Liu, X. Y. Tao, Biomacromolecules enabled dendrite-free lithium metal battery and its origin revealed by cryo-electron microscopy. *Nat. Commun.* **11**, 488 (2020).
55. D. Zhang, Y. Yin, C. Liu, S. Fan, Modified secondary lithium metal batteries with the polyaniline-carbon nanotube composite buffer layer. *Chem. Commun.* **51**, 322–325 (2015).
56. R. Xu, X.-Q. Zhang, X.-B. Cheng, H.-J. Peng, C.-Z. Zhao, C. Yan, J.-Q. Huang, Artificial soft-rigid protective layer for dendrite-free lithium metal anode. *Adv. Funct. Mater.* **28**, 1705838 (2018).
57. M. S. Kim, M.-S. Kim, Y. Do, Y. R. Lim, I. W. Nah, L. A. Archer, W. I. Cho, Designing solid-electrolyte interphases for lithium sulfur electrodes using ionic shields. *Nano Energy* **41**, 573–582 (2017).
58. H. Xu, S. Li, C. Zhang, X. Chen, W. Liu, Y. Zheng, Y. Xie, Y. Huang, J. Li, Roll-to-roll prelithiation of Sn foil anode suppresses gassing and enables stable full-cell cycling of lithium ion batteries. *Energ. Environ. Sci.* **12**, 2991–3000 (2019).
59. H. Wang, D. Lin, Y. Y. Liu, Y. Li, Y. Cui, Ultrahigh-current density anodes with interconnected Li metal reservoir through overlithiation of mesoporous  $\text{AlF}_3$  framework. *Sci. Adv.* **3**, e1701301 (2017).
60. M. Wan, S. Kang, L. Wang, H. W. Lee, G. W. Zheng, Y. Cui, Y. Sun, Mechanical rolling formation of interpenetrated lithium metal/lithium tin alloy foil for ultrahigh-rate battery anode. *Nat. Commun.* **11**, 829 (2020).
61. S. Liu, X. Ji, J. Yue, S. Hou, P. Wang, C. Cui, J. Chen, B. Shao, J. Li, F. Han, J. Tu, C. Wang, High interfacial-energy interphase promoting safe lithium metal batteries. *J. Am. Chem. Soc.* **142**, 2438–2447 (2020).
62. Z. Peng, N. Zhao, Z. Zhang, H. Wan, H. Lin, M. Liu, C. Shen, H. He, X. Guo, J.-G. Zhang, D. Wang, Stabilizing Li/electrolyte interface with a transplantable protective layer based on nanoscale LiF domains. *Nano Energy* **39**, 662–672 (2017).
63. X. Shen, Y. Li, T. Qian, J. Liu, J. Zhou, C. Yan, J. B. Goodenough, Lithium anode stable in air for low-cost fabrication of a dendrite-free lithium battery. *Nat. Commun.* **10**, 900 (2019).
64. Y. Yu, G. Huang, J. Z. Wang, K. Li, J. L. Ma, X. B. Zhang, In situ designing a gradient  $\text{Li}^+$  capture and quasi-spontaneous diffusion anode protection layer toward long-life  $\text{Li-O}_2$  batteries. *Adv. Mater.* **32**, 2004157 (2020).
65. S. Sun, S. Myung, G. Kim, D. Lee, H. Son, M. Jang, E. Park, B. Son, Y. Jung, U. Paik, T. Song, Facile ex situ formation of a LiF-polymer composite layer as an artificial SEI layer on Li metal by simple roll-press processing for carbonate electrolyte-based Li metal batteries. *J. Mater. Chem. A* **8**, 17229–17237 (2020).
66. Y. He, Y. Zhang, Z. Wang, X. Li, Z. Lü, X. Huang, Z. Liu, In situ surface film formed by solid-state anodic oxidation for stable lithium metal anodes. *Adv. Funct. Mater.* **31**, 2101737 (2021).
67. S. Ye, L. Wang, F. Liu, P. Shi, H. Wang, X. Wu, Y. Yu,  $\text{g-C}_3\text{N}_4$  derivative artificial organic/inorganic composite solid electrolyte interphase layer for stable lithium metal anode. *Adv. Energy Mater.* **10**, 2002647 (2020).
68. D. Lee, S. Sun, J. Kwon, H. Park, M. Jang, E. Park, B. Son, Y. Jung, T. Song, U. Paik, Copper nitride nanowires printed Li with stable cycling for Li metal batteries in carbonate electrolytes. *Adv. Mater.* **32**, 1905573 (2020).
69. Z. Luo, S. Li, L. Yang, Y. Tian, L. Xu, G. Zou, H. Hou, W. Wei, L. Chen, X. Ji, Interfacially redistributed charge for robust lithium metal anode. *Nano Energy* **87**, 106212 (2021).
70. C. Yan, R. Xu, Y. Xiao, J.-F. Ding, L. Xu, B.-Q. Li, J.-Q. Huang, Toward critical electrode/electrolyte interfaces in rechargeable batteries. *Adv. Funct. Mater.* **30**, 1909887 (2020).
71. Q. Zhang, P. Y. Chen, C. Yan, P. Chen, R. Zhang, Y. X. Yao, H. J. Peng, L. T. Yan, S. Kaskel, Selective permeable lithium-ion channels on lithium metal for practical lithium-sulfur pouch cells. *Angew. Chem. Int. Ed.* **133**, 18179–18184 (2021).
72. Z. Takehara, Z. Ogumi, Y. Uchimoto, K. Yasuda, H. Yoshida, Modification of lithium/electrolyte interface by plasma polymerization of 1,1-difluoroethene. *J. Power Sources* **43-44**, 377–383 (1993).
73. J. Zhao, M. Hong, Z. Ju, X. Yan, Y. Gai, Z. Liang, Durable lithium metal anodes enabled by interfacial layers based on mechanically interlocked networks capable of energy dissipation. *Angew. Chem. Int. Ed.* **61**, e202214386 (2022).
74. Y. Gao, Y. Zhao, Y. C. Li, Q. Huang, T. E. Mallouk, D. Wang, Interfacial chemistry regulation via a skin-grafting strategy enables high-performance lithium-metal batteries. *J. Am. Chem. Soc.* **139**, 15288–15291 (2017).

75. J. Wu, Z. Rao, X. Liu, Y. Shen, C. Fang, L. Yuan, Z. Li, W. Zhang, X. Xie, Y. Huang, Polycationic polymer layer for air-stable and dendrite-free Li metal anodes in carbonate electrolytes. *Adv. Mater.* **33**, 2007428 (2021).
76. Q. Yang, J. Hu, J. Meng, C. Li, C–F-rich oil drop as a non-expendable fluid interface modifier with low surface energy to stabilize a Li metal anode. *Energ. Environ. Sci.* **14**, 3621–3631 (2021).
77. Y. Xiao, R. Xu, C. Yan, Y. Liang, J.-F. Ding, J.-Q. Huang, Waterproof lithium metal anode enabled by cross-linking encapsulation. *Sci. Bull.* **65**, 909 (2020).
78. Z. Zhou, Y. Feng, J. Wang, B. Liang, Y. Li, Z. Song, D. M. Itkis, J. Song, A robust, highly stretchable ion-conductive skin for stable lithium metal batteries. *Chem. Eng. J.* **396**, 125254 (2020).
79. Y. Yao, X. Zhao, A. A. Razzaq, Y. Gu, X. Yuan, R. Shah, Y. Lian, J. Lei, Q. Mu, Y. Ma, Y. Peng, Z. Deng, Z. Liu, Mosaic rGO layers on lithium metal anodes for the effective mediation of lithium plating and stripping. *J. Mater. Chem. A* **7**, 12214–12224 (2019).
80. W. Liu, Y. Xia, W. Wang, Y. Wang, J. Jin, Y. Chen, E. Paek, D. Mitlin, Pristine or highly defective? Understanding the role of graphene structure for stable lithium metal plating. *Adv. Energy Mater.* **9**, 1802918 (2018).
81. Y. T. Chen, S. A. Abbas, N. Kaiser, S. H. Wu, H. A. Chen, K. M. Boopathi, M. Singh, J. Fang, C. W. Pao, C. W. Chu, Mitigating metal dendrite formation in lithium-sulfur batteries via morphology-tunable graphene oxide interfaces. *ACS Appl. Mater. Inter.* **11**, 2060–2070 (2019).
82. H. Zhang, X. Liao, Y. Guan, Y. Xiang, M. Li, W. Zhang, X. Zhu, H. Ming, L. Lu, J. Qiu, Y. Huang, G. Cao, Y. Yang, L. Mai, Y. Zhao, H. Zhang, Lithiophilic-lithiophobic gradient interfacial layer for a highly stable lithium metal anode. *Nat. Commun.* **9**, 3729 (2018).
83. D. J. Lee, H. Lee, Y. J. Kim, J. K. Park, H. T. Kim, Sustainable redox mediation for lithium-oxygen batteries by a composite protective layer on the lithium-metal anode. *Adv. Mater.* **28**, 857–863 (2016).
84. W.-J. Kwak, S.-J. Park, H.-G. Jung, Y.-K. Sun, Optimized concentration of redox mediator and surface protection of Li metal for maintenance of high energy efficiency in Li-O<sub>2</sub> batteries. *Adv. Energy Mater.* **8**, 1702258 (2018).
85. G. Jiang, K. Li, F. Yu, X. Li, J. Mao, W. Jiang, F. Sun, B. Dai, Y. Li, Robust artificial solid-electrolyte interfaces with biomimetic ionic channels for dendrite-free Li metal anodes. *Adv. Energy Mater.* **11**, 2003496 (2021).
86. L. Fan, Z. Guo, Y. Zhang, X. Wu, C. Zhao, X. Sun, G. Yang, Y. Feng, N. Zhang, Stable artificial solid electrolyte interphase films for lithium metal anode via metal-organic frameworks cemented by polyvinyl alcohol. *J. Mater. Chem. A* **8**, 251–258 (2020).
87. X. Li, Y. Tian, L. Shen, Z. Qu, T. Ma, F. Sun, X. Liu, C. Zhang, J. Shen, X. Li, L. Gao, S. Xiao, T. Liu, Y. Liu, Y. F. Lu, Electrolyte interphase built from anionic covalent organic frameworks for lithium dendrite suppression. *Adv. Funct. Mater.* **31**, 2009718 (2021).
88. Z. Wang, Y. Wang, Z. Zhang, X. Chen, W. Lie, Y.-B. He, Z. Zhou, G. Xia, Z. Guo, Building artificial solid-electrolyte interphase with uniform intermolecular ionic bonds toward dendrite-free lithium metal anodes. *Adv. Funct. Mater.* **30**, 2002414 (2020).
89. X. Zhang, Q. Zhang, X. G. Wang, C. Wang, Y. N. Chen, Z. Xie, Z. Zhou, An extremely simple method for protecting lithium anodes in Li-O<sub>2</sub> batteries. *Angew. Chem. Int. Ed.* **57**, 12814–12818 (2018).
90. P. Gao, C. Zhang, G. Wen, Equivalent circuit model analysis on electrochemical impedance spectroscopy of lithium metal batteries. *J. Power Sources* **294**, 67–74 (2015).
91. N. D. Trinh, D. Lepage, D. Ayme-Perrot, A. Badia, M. Dolle, D. Rochefort, An artificial lithium protective layer that enables the use of acetonitrile-based electrolytes in lithium metal batteries. *Angew. Chem. Int. Ed.* **57**, 5072–5075 (2018).
92. C. Yan, X. B. Cheng, Y. Tian, X. Chen, X. Q. Zhang, W. J. Li, J. Q. Huang, Q. Zhang, Dual-layered film protected lithium metal anode to enable dendrite-free lithium deposition. *Adv. Mater.* **30**, 1707629 (2018).
93. X. Liu, J. Liu, T. Qian, H. Chen, C. Yan, Novel organophosphate-derived dual-layered interface enabling air-stable and dendrite-free lithium metal anode. *Adv. Mater.* **32**, 1902724 (2020).
94. N. W. Li, Y. Shi, Y. X. Yin, X. X. Zeng, J. Y. Li, C. J. Li, L. J. Wan, R. Wen, Y. G. Guo, A flexible solid electrolyte interphase layer for long-life lithium metal anodes. *Angew. Chem. Int. Ed.* **57**, 1505–1509 (2018).
95. G. Wang, C. Chen, Y. Chen, X. Kang, C. Yang, F. Wang, Y. Liu, X. Xiong, Self-stabilized and strongly adhesive supramolecular polymer protective layer enables ultrahigh-rate and large-capacity lithium-metal anode. *Angew. Chem. Int. Ed.* **59**, 2055–2060 (2020).
96. C. Chen, Q. Liang, G. Wang, D. Liu, X. Xiong, Grain-boundary-rich artificial SEI layer for high-rate lithium metal anodes. *Adv. Funct. Mater.* **32**, 2107249 (2021).
97. M. Bai, K. Xie, K. Yuan, K. Zhang, N. Li, C. Shen, Y. Lai, R. Vajtai, P. Ajayan, B. Wei, A scalable approach to dendrite-free lithium anodes via spontaneous reduction of spray-coated graphene oxide layers. *Adv. Mater.* **30**, 1801213 (2018).
98. Y. L. Cui, S. F. Liu, D. H. Wang, X. L. Wang, X. H. Xia, C. D. Gu, J. P. Tu, A facile way to construct stable and ionic conductive lithium sulfide nanoparticles composed solid electrolyte interphase on Li metal anode. *Adv. Funct. Mater.* **31**, 2006380 (2020).
99. J. Liang, X. Li, Y. Zhao, L. V. Goncharova, G. Wang, K. R. Adair, C. Wang, R. Li, Y. Zhu, Y. Qian, L. Zhang, R. Yang, S. Lu, X. Sun, In situ Li<sub>2</sub>PS<sub>4</sub> solid-state electrolyte protection layers for superior long-life and high-rate lithium-metal anodes. *Adv. Mater.* **30**, 1804684 (2018).
100. H. Su, Y. Liu, Y. Zhong, J. Li, X. Wang, X. Xia, C. Gu, J. Tu, Stabilizing the interphase between Li and argyrodite electrolyte through synergistic phosphating process for all-solid-state lithium batteries. *Nano Energy* **96**, 107104 (2022).
101. X. Liang, Q. Pang, I. R. Kochetkov, M. S. Sempere, H. Huang, X. Sun, L. F. Nazar, A facile surface chemistry route to a stabilized lithium metal anode. *Nat. Energy* **2**, 17119 (2017).
102. T. Chen, W. Kong, P. Zhao, H. Lin, Y. Hu, R. Chen, W. Yan, Z. Jin, Dendrite-free and stable lithium metal anodes enabled by an antimony-based lithiophilic interphase. *Chem. Mater.* **31**, 7565–7573 (2019).
103. A. Hu, W. Chen, X. Du, Y. Hu, T. Lei, H. Wang, L. Xue, Y. Li, H. Sun, Y. Yan, J. Long, C. Shu, J. Zhu, B. Li, X. Wang, J. Xiong, An artificial hybrid interphase for an ultrahigh-rate and practical lithium metal anode. *Energ. Environ. Sci.* **14**, 4115–4124 (2021).
104. W. Guo, Q. Han, J. Jiao, W. Wu, X. Zhu, Z. Chen, Y. Zhao, In situ construction of robust biphasic surface layers on lithium metal for lithium-sulfide batteries with long cycle life. *Angew. Chem. Int. Ed.* **60**, 7267–7274 (2021).
105. C. Wei, L. Tan, Y. Tao, Y. An, Y. Tian, H. Jiang, J. Feng, Y. Qian, Interfacial passivation by room-temperature liquid metal enabling stable 5 V-class lithium-metal batteries in commercial carbonate-based electrolyte. *Energy Storage Mater.* **34**, 12–21 (2021).
106. L. Lin, L. Suo, Y. Hu, H. Li, X. Huang, L. Chen, Epitaxial induced plating current-collector lasting lifespan of anode-free lithium metal battery. *Adv. Energy Mater.* **11**, 2003709 (2021).
107. Q. Jin, X. Zhang, H. Gao, L. Li, Z. Zhang, Novel Li<sub>2</sub>Si<sub>2</sub>/nafion as an artificial SEI film to enable dendrite-free Li metal anodes and high stability Li-S batteries. *J. Mater. Chem. A* **8**, 8979–8988 (2020).
108. Y. Zhao, G. Li, Y. Gao, D. Wang, Q. Huang, D. Wang, Stable Li metal anode by a hybrid lithium polysulfidophosphate/polymer cross-linking film. *ACS Energy Lett.* **4**, 1271–1278 (2019).
109. Q. Zhao, Z. Y. Tu, S. Wei, K. H. Zhang, S. Choudhury, X. Liu, L. A. Archer, Building organic/inorganic hybrid interphases for fast interfacial transport in rechargeable metal batteries. *Angew. Chem. Int. Ed.* **130**, 1004–1008 (2018).
110. Y. Gao, Z. Yan, J. L. Gray, X. He, D. Wang, T. Chen, Q. Huang, Y. C. Li, H. Wang, S. H. Kim, T. E. Mallouk, D. Wang, Polymer-inorganic solid-electrolyte interphase for stable lithium metal batteries under lean electrolyte conditions. *Nat. Mater.* **18**, 384–389 (2019).
111. K. Yan, J. Wang, S. Zhao, D. Zhou, B. Sun, Y. Cui, G. Wang, Temperature-dependent nucleation and growth of dendrite-free lithium metal anodes. *Angew. Chem. Int. Ed.* **58**, 11364–11368 (2019).
112. Y. Gu, W. W. Wang, Y. J. Li, Q. H. Wu, S. Tang, J. W. Yan, M. S. Zheng, D. Y. Wu, C. H. Fan, W. Q. Hu, Z. B. Chen, Y. Fang, Q. H. Zhang, Q. F. Dong, B. W. Mao, Designable ultra-smooth ultra-thin solid-electrolyte interphases of three alkali metal anodes. *Nat. Commun.* **9**, 1339 (2018).
113. W. W. Wang, Y. Gu, H. Yan, S. Li, J.-W. He, H.-Y. Xu, Q.-H. Wu, J.-W. Yan, B.-W. Mao, Evaluating solid-electrolyte interphases for lithium and lithium-free anodes from nanoindentation features. *Chem* **6**, 2728–2745 (2020).
114. X.-D. Lin, Y. Gu, X.-R. Shen, W.-W. Wang, Y.-H. Hong, Q.-H. Wu, Z.-Y. Zhou, D.-Y. Wu, J.-K. Chang, M.-S. Zheng, B.-W. Mao, Q.-F. Dong, An oxygen-blocking oriented multifunctional solid-electrolyte interphase as a protective layer for a lithium metal anode in lithium-oxygen batteries. *Energ. Environ. Sci.* **14**, 1439–1448 (2021).
115. Y.-K. Huang, R. Pan, D. Rehnlund, Z. Wang, L. Nyholm, First-cycle oxidative generation of lithium nucleation sites stabilizes lithium-metal electrodes. *Adv. Energy Mater.* **11**, 2003674 (2021).
116. B. Liu, W. Xu, J. Tao, P. Yan, J. Zheng, M. H. Engelhard, D. Lu, C. Wang, J.-G. Zhang, Enhanced cyclability of lithium-oxygen batteries with electrodes protected by surface films induced via in situ electrochemical process. *Adv. Energy Mater.* **8**, 1702340 (2018).
117. G. Hou, X. Ma, Q. Sun, Q. Ai, X. Xu, L. Chen, D. Li, J. Chen, H. Zhong, Y. Li, Z. Xu, P. Si, J. Feng, L. Zhang, F. Ding, L. Ci, Lithium dendrite suppression and enhanced interfacial compatibility enabled by an ex situ SEI on Li anode for LAGP-based all-solid-state batteries. *ACS Appl. Mater. Inter.* **10**, 18610–18618 (2018).
118. Y. Gao, D. Wang, Y. C. Li, Z. Yu, T. E. Mallouk, D. Wang, Salt-based organic-inorganic nanocomposites: Towards a stable lithium metal/Li<sub>10</sub>GeP<sub>2</sub>S<sub>12</sub> solid electrolyte interface. *Angew. Chem. Int. Ed.* **57**, 13608–13612 (2018).
119. X.-B. Cheng, C. Yan, X. Chen, C. Guan, J.-Q. Huang, H.-J. Peng, R. Zhang, S.-T. Yang, Q. Zhang, Implantable solid electrolyte interphase in lithium-metal batteries. *Chem* **2**, 258–270 (2017).

120. G. Lu, J. Nai, H. Yuan, J. Wang, J. Zheng, Z. Ju, C. Jin, Y. Wang, T. Liu, Y. Liu, X. Tao, In-situ electrodeposition of nanostructured carbon strengthened interface for stabilizing lithium metal anode. *ACS Nano* **16**, 9883–9893 (2022).
121. Y. Ma, L. Li, J. Qian, W. Qu, R. Luo, F. Wu, R. Chen, Materials and structure engineering by magnetron sputtering for advanced lithium batteries. *Energy Storage Mater.* **39**, 203–224 (2021).
122. D. C. Lin, Y. Y. Liu, W. Chen, G. M. Zhou, K. Liu, B. Dunn, Y. Cui, Conformal lithium fluoride protection layer on three-dimensional lithium by nonhazardous gaseous reagent freon. *Nano Lett.* **17**, 3731–3737 (2017).
123. W. Tang, X. Yin, S. Kang, Z. Chen, B. Tian, S. L. Teo, X. Wang, X. Chi, K. P. Loh, H. W. Lee, G. W. Zheng, Lithium silicide surface enrichment: A solution to lithium metal battery. *Adv. Mater.* **30**, 1801745 (2018).
124. R. Pathak, K. Chen, A. Gurung, K. M. Reza, B. Bahrami, F. Wu, A. Chaudhary, N. Ghimire, B. Zhou, W.-H. Zhang, Y. Zhou, Q. Qiao, Ultrathin bilayer of graphite/SiO<sub>2</sub> as solid interface for reviving Li metal anode. *Adv. Energy Mater.* **9**, 1901486 (2019).
125. L. Fan, H. L. Zhuang, L. Gao, Y. Y. Lu, L. A. Archer, Regulating Li deposition at artificial solid electrolyte interphases. *J. Mater. Chem. A* **5**, 3483–3492 (2017).
126. E. Cha, M. D. Patel, J. Park, J. Hwang, V. Prasad, K. Cho, W. Choi, 2D MoS<sub>2</sub> as an efficient protective layer for lithium metal anodes in high-performance Li-S batteries. *Nat. Nanotechnol.* **13**, 337–344 (2018).
127. P. Li, W. Feng, X. Dong, Y. Wang, Y. Xia, A new strategy of constructing a highly fluorinated solid-electrolyte interface towards high-performance lithium anode. *Adv. Mater. Inter.* **7**, 2000154 (2020).
128. Q. Li, H. Pan, W. Li, Y. Wang, J. Wang, J. Zheng, X. Yu, H. Li, L. Chen, Homogeneous interface conductivity for lithium dendrite-free anode. *ACS Energy Lett.* **3**, 2259–2266 (2018).
129. L. Wang, Q. Wang, W. Jia, S. Chen, P. Gao, J. Li, Li metal coated with amorphous Li<sub>3</sub>PO<sub>4</sub> via magnetron sputtering for stable and long-cycle life lithium metal batteries. *J. Power Sources* **342**, 175–182 (2017).
130. C. Gao, Q. Dong, G. Zhang, H. Fan, H. Li, B. Hong, Y. Lai, Antimony-doped lithium phosphate artificial solid electrolyte interphase for dendrite-free lithium-metal batteries. *ChemElectroChem* **6**, 1134–1138 (2019).
131. K. K. Fu, Y. Gong, Z. Fu, H. Xie, Y. Yao, B. Liu, M. Carter, E. Wachsman, L. Hu, Transient behavior of the metal interface in lithium metal-garnet batteries. *Angew. Chem. Int. Ed.* **56**, 14942–14947 (2017).
132. X. Hao, Q. Zhao, S. Su, S. Zhang, J. Ma, L. Shen, Q. Yu, L. Zhao, Y. Liu, F. Kang, Y.-B. He, Constructing multifunctional interphase between Li<sub>1.4</sub>Al<sub>0.4</sub>Ti<sub>1.6</sub>(PO<sub>4</sub>)<sub>3</sub> and Li metal by magnetron sputtering for highly stable solid-state lithium metal batteries. *Adv. Energy Mater.* **9**, 1901604 (2019).
133. Y. J. Zhang, X. Y. Liu, W. Q. Bai, H. Tang, S. J. Shi, X. L. Wang, C. D. Gu, J. P. Tu, Magnetron sputtering amorphous carbon coatings on metallic lithium: Towards promising anodes for lithium secondary batteries. *J. Power Sources* **266**, 43–50 (2014).
134. T. Chen, F. Meng, Z. Zhang, J. Liang, Y. Hu, W. Kong, X. L. Zhang, Z. Jin, Stabilizing lithium metal anode by molecular beam epitaxy grown uniform and ultrathin bismuth film. *Nano Energy* **76**, 105068 (2020).
135. K. Yan, H. W. Lee, T. Gao, G. Zheng, H. Yao, H. Wang, Z. Lu, Y. Zhou, Z. Liang, Z. Liu, S. Chu, Y. Cui, Ultrathin two-dimensional atomic crystals as stable interfacial layer for improvement of lithium metal anode. *Nano Lett.* **14**, 6016–6022 (2014).
136. Q. Xu, J. Lin, C. Ye, X. Jin, D. Ye, Y. Lu, G. Zhou, Y. Qiu, W. Li, Air-stable and dendrite-free lithium metal anodes enabled by a hybrid interphase of C60 and Mg. *Adv. Energy Mater.* **10**, 1903292 (2019).
137. S. Stalin, P. Chen, G. Li, Y. Deng, Z. Rouse, Y. Cheng, Z. Zhang, P. Biswal, S. Jin, S. P. Baker, R. Yang, L. A. Archer, Ultrathin zwitterionic polymeric interphases for stable lithium metal anodes. *Matter* **4**, 3753–3773 (2021).
138. J. Y. Kim, A. Y. Kim, G. Liu, J. Y. Woo, H. Kim, J. K. Lee, Li<sub>4</sub>SiO<sub>4</sub>-based artificial passivation thin film for improving interfacial stability of Li metal anodes. *ACS Appl. Mater. Inter.* **10**, 8692–8701 (2018).
139. Y. Zhao, K. Zheng, X. L. Sun, Addressing interfacial issues in liquid-based and solid-state batteries by atomic and molecular layer deposition. *Joule* **2**, 2583–2604 (2018).
140. J. Xie, L. Liao, Y. Gong, Y. Li, F. Shi, A. Pei, J. Sun, R. Zhang, B. Kong, R. Subbaraman, J. Christensen, Y. Cui, Stitching h-BN by atomic layer deposition of LiF as a stable interface for lithium metal anode. *Sci. Adv.* **3**, eaao3170 (2017).
141. M. Wang, X. Cheng, T. Cao, J. Niu, R. Wu, X. Liu, Y. Zhang, Constructing ultrathin TiO<sub>2</sub> protection layers via atomic layer deposition for stable lithium metal anode cycling. *J. Alloy. Compd.* **865**, 158748 (2021).
142. P. K. Alaboina, S. Rodrigues, M. Rottmayer, S. J. Cho, In situ dendrite suppression study of nanolayer encapsulated Li metal enabled by zirconia atomic layer deposition. *ACS Appl. Mater. Inter.* **10**, 32801–32808 (2018).
143. A. C. Kozen, C. F. Lin, A. J. Pearse, M. A. Schroeder, X. Han, L. Hu, S. B. Lee, G. W. Rubloff, M. Noked, Next-generation lithium metal anode engineering via atomic layer deposition. *ACS Nano* **9**, 5884–5892 (2015).
144. Y. Zhao, X. L. Sun, Molecular layer deposition for energy conversion and storage. *ACS Energy Lett.* **3**, 899–914 (2018).
145. C. Wang, Y. Zhao, Q. Sun, X. Li, Y. Liu, J. Liang, X. Li, X. Lin, R. Li, K. R. Adair, L. Zhang, R. Yang, S. Lu, X. Sun, Stabilizing interface between Li<sub>10</sub>SnP<sub>2</sub>S<sub>12</sub> and Li metal by molecular layer deposition. *Nano Energy* **53**, 168–174 (2018).
146. Y. P. Sun, Y. Zhao, J. Wang, J. Liang, C. Wang, Q. Sun, X. Lin, K. R. Adair, J. Luo, D. Wang, R. Li, M. Cai, T. K. Sham, X. L. Sun, A novel organic "polyurea" thin film for ultralong-life lithium-metal anodes via molecular-layer deposition. *Adv. Mater.* **31**, 1806541 (2019).
147. Y. Sun, M. Amirmaleki, Y. Zhao, C. Zhao, J. Liang, C. Wang, K. R. Adair, J. Li, T. Cui, G. Wang, R. Li, T. Filleter, M. Cai, T.-K. Sham, X. L. Sun, Tailoring the mechanical and electrochemical properties of an artificial interphase for high-performance metallic lithium anode. *Adv. Energy Mater.* **10**, 2001139 (2020).
148. Y. Sun, C. Zhao, K. R. Adair, Y. Zhao, L. V. Goncharova, J. Liang, C. Wang, J. Li, R. Li, M. Cai, T.-K. Sham, X. Sun, Regulated lithium plating and stripping by a nano-scale gradient inorganic-organic coating for stable lithium metal anodes. *Energ. Environ. Sci.* **14**, 4085–4094 (2021).
149. Y. Zhao, M. Amirmaleki, Q. Sun, C. Zhao, A. Codireni, L. V. Goncharova, C. Wang, K. Adair, X. Li, X. Yang, F. Zhao, R. Li, T. Filleter, M. Cai, X. Sun, Natural SEI-inspired dual-protective layers via atomic/molecular layer deposition for long-life metallic lithium anode. *Matter* **1**, 1215–1231 (2019).
150. J. Zhao, L. Liao, F. Shi, T. Lei, G. Chen, A. Pei, J. Sun, K. Yan, G. Zhou, J. Xie, C. Liu, Y. Li, Z. Liang, Z. Bao, Y. Cui, Surface fluorination of reactive battery anode materials for enhanced stability. *J. Am. Chem. Soc.* **139**, 11550–11558 (2017).
151. Y. Li, Y. Sun, A. Pei, K. Chen, A. Vailionis, Y. Li, G. Zheng, J. Sun, Y. Cui, Robust pinhole-free Li<sub>3</sub>N solid electrolyte grown from molten lithium. *ACS Cent. Sci.* **4**, 97–104 (2018).
152. Y. Lin, Z. Wen, J. Liu, D. Wu, P. Zhang, J. Zhao, Constructing a uniform lithium iodide layer for stabilizing lithium metal anode. *J. Energy Chem.* **55**, 129–135 (2021).
153. Y. Nan, S. Li, M. Zhu, B. Li, S. Yang, Endowing lithium metal surface with self-healing property via an in situ gas-solid reaction for high-performance lithium metal batteries. *ACS Appl. Mater. Inter.* **11**, 28878–28884 (2019).
154. H. Chen, A. Pei, D. Lin, J. Xie, A. Yang, J. Xu, K. Lin, J. Wang, H. Wang, F. Shi, D. Boyle, Y. Cui, Uniform high ionic conducting lithium sulfide protection layer for stable lithium metal anode. *Adv. Energy Mater.* **9**, 1900858 (2019).
155. F. Liu, L. Wang, Z. Zhang, P. Shi, Y. Feng, Y. Yao, S. Ye, H. Wang, X. Wu, Y. Yu, A mixed lithium-ion conductive Li<sub>2</sub>S/Li<sub>2</sub>Se protection layer for stable lithium metal anode. *Adv. Funct. Mater.* **30**, 2001607 (2020).
156. H. F. Zandy, Plasma: The fourth state of matter. *The Physics Teacher* **8**, 27–31 (1970).
157. J. Zheng, R. Yang, L. Xie, J. Qu, Y. Liu, X. Li, Plasma-assisted approaches in inorganic nanostructure fabrication. *Adv. Mater.* **22**, 1451–1473 (2010).
158. H. F. Liang, F. W. Ming, H. N. Alshareef, Applications of plasma in energy conversion and storage materials. *Adv. Energy Mater.* **8**, 1801804 (2018).
159. K. Chen, R. Pathak, A. Gurung, E. A. Adhamash, B. Bahrami, Q. He, H. Qiao, A. L. Smirnova, J. J. Wu, Q. Qiao, Y. Zhou, Flower-shaped lithium nitride as a protective layer via facile plasma activation for stable lithium metal anodes. *Energy Storage Mater.* **18**, 389–396 (2019).
160. S. Cao, X. He, L. Nie, J. Hu, M. Chen, Y. Han, K. Wang, K. Jiang, M. Zhou, CF<sub>4</sub> plasma-generated LiF-Li<sub>2</sub>C<sub>2</sub> artificial layers for dendrite-free lithium-metal anodes. *Adv. Sci.* **9**, 2201147 (2022).
161. X. Jin, Z. Cai, X. Zhang, J. Yu, Q. He, Z. Lu, M. Dahbi, J. Alami, J. Lu, K. Amine, H. Zhang, Transferring liquid metal to form a hybrid solid electrolyte via a wettability-tuning technology for lithium-metal anodes. *Adv. Mater.* **34**, e2200181 (2022).
162. K. Liu, A. Pei, H. R. Lee, B. Kong, N. Liu, D. Lin, Y. Liu, C. Liu, P. C. Hsu, Z. Bao, Y. Cui, Lithium metal anodes with an adaptive "solid-liquid" interfacial protective layer. *J. Am. Chem. Soc.* **139**, 4815–4820 (2017).
163. H. D. Yuan, J. W. Nai, H. Tian, Z. J. Ju, W. K. Zhang, Y. J. Liu, X. Y. Tao, X. W. Lou, An ultrastable lithium metal anode enabled by designed metal fluoride spansules. *Sci. Adv.* **6**, eaaz3112 (2020).
164. Y. Gao, T. Rojas, K. Wang, S. Liu, D. Wang, T. Chen, H. Wang, A. T. Ngo, D. Wang, Low-temperature and high-rate-charging lithium metal batteries enabled by an electrochemically active monolayer-regulated interface. *Nat. Energy* **5**, 534–542 (2020).
165. X. Wei, X. Wang, Q. An, C. Han, L. Q. Mai, Operando X-ray diffraction characterization for understanding the intrinsic electrochemical mechanism in rechargeable battery materials. *Small Methods* **1**, 1700083 (2017).
166. S. Mourdikoudis, R. M. Pallares, N. T. K. Thanh, Characterization techniques for nanoparticles: Comparison and complementarity upon studying nanoparticle properties. *Nanoscale* **10**, 12871–12934 (2018).



167. Z. Shadike, E. Zhao, Y.-N. Zhou, X. Yu, Y. Yang, E. Hu, S. Bak, L. Gu, X.-Q. Yang, Advanced characterization techniques for sodium-ion battery studies. *Adv. Energy Mater.* **8**, 1702588 (2018).
168. R. Xu, J. Lu, K. Amine, Progress in mechanistic understanding and characterization techniques of Li-S batteries. *Adv. Energy Mater.* **5**, 1500408 (2015).
169. H. Park, O. Tamwattana, J. Kim, S. Buakeaw, R. Hongtong, B. Kim, P. Khomein, G. Liu, N. Meethong, K. Kang, Probing lithium metals in batteries by advanced characterization and analysis tools. *Adv. Energy Mater.* **11**, 2003039 (2020).
170. Y. Xu, K. Dong, Y. Jie, P. Adelhelm, Y. Chen, L. Xu, P. Yu, J. Kim, Z. Kochovski, Z. Yu, W. Li, J. LeBeau, Y. Shao-Horn, R. Cao, S. Jiao, T. Cheng, I. Manke, Y. Lu, Promoting mechanistic understanding of lithium deposition and solid-electrolyte interphase (SEI) formation using advanced characterization and simulation methods: Recent progress, limitations, and future perspectives. *Adv. Energy Mater.* **12**, 2200398 (2022).
171. X. Q. Zhang, X. Chen, X. B. Cheng, B. Q. Li, X. Shen, C. Yan, J. Q. Huang, Q. Zhang, Highly stable lithium metal batteries enabled by regulating the solvation of lithium ions in nonaqueous electrolytes. *Angew. Chem. Int. Ed.* **57**, 5301–5305 (2018).
172. Y. Li, K. Wang, W. Zhou, Y. Li, R. Vila, W. Huang, H. Wang, G. Chen, G.-H. Wu, Y. Tsao, H. Wang, R. Sinclair, W. Chiu, Y. Cui, Cryo-EM structures of atomic surfaces and host-guest chemistry in metal-organic frameworks. *Matter* **1**, 428–438 (2019).
173. Y. Li, Y. Li, A. Pei, K. Yan, Y. Sun, C.-L. Wu, L.-M. Joubert, R. Chin, A. L. Koh, Y. Yu, J. Perrino, B. Butz, S. Chu, Y. Cui, Atomic structure of sensitive battery materials and interfaces revealed by cryo-electron microscopy. *Science* **358**, 506–510 (2017).
174. H. Yuan, J. Nai, Y. Fang, G. Lu, X. Tao, X. W. D. Lou, Double-shelled C@MoS<sub>2</sub> structures preloaded with sulfur: An additive reservoir for stable lithium metal anodes. *Angew. Chem. Int. Ed.* **59**, 15839–15843 (2020).
175. O. W. Sheng, J. H. Zheng, Z. J. Ju, C. B. Jin, Y. Wang, M. Chen, J. W. Nai, T. F. Liu, W. K. Zhang, Y. J. Liu, X. Y. Tao, In situ construction of a LiF-enriched interface for stable all-solid-state batteries and its origin revealed by cryo-TEM. *Adv. Mater.* **32**, 2000223 (2020).
176. O. W. Sheng, C. B. Jin, Z. J. Ju, J. H. Zheng, T. F. Liu, Y. J. Liu, Y. Wang, J. M. Luo, X. Y. Tao, J. W. Nai, Stabilizing Li<sub>2</sub>SnS<sub>4</sub> electrolyte from interface to bulk phase with a gradient lithium iodide/polymer layer in lithium metal batteries. *Nano Lett.* **22**, 8346–8354 (2022).
177. A. Dazzi, F. Glotin, R. Carminati, Theory of infrared nanospectroscopy by photothermal induced resonance. *J. Appl. Phys.* **107**, 124519 (2010).
178. F. Lu, M. Jin, M. A. Belkin, Tip-enhanced infrared nanospectroscopy via molecular expansion force detection. *Nat. Photonics* **8**, 307–312 (2014).

#### Acknowledgments

**Funding:** This work is supported by the funding of the National Key R&D Program of China (2022YFB2502000), the "Leading Innovative and Entrepreneur Team Introduction Program of Zhejiang" (2020R01002), and the National Natural Science Foundation of China (grant nos. 52225208, 51972285, and U21A20174). **Author contributions:** G.L., J.N., D.L., X.T., and X.W.L. conceived the topic of this review. G.L. and J.N. cowrote the initial draft. X.T. and X.W.L. supervised the writing of the manuscript and made revisions. **Competing interests:** The authors declare that they have no competing interests. **Data and materials availability:** All data needed to evaluate the conclusions in the paper are present in the paper.

Submitted 3 October 2022

Accepted 7 March 2023

Published 5 April 2023

10.1126/sciadv.adf1550